DTU Technical University of Denmark

KØBENHAVNS UNIVERSITET

Organ-on-a-chip system to quantify cellular internalization and transport across the intestinal barrier of lipidated salmon calcitonin analogs using fluorescence microscopy

Emilie Kok

Master thesis, August 2021

Master in Nanoscience

Supervisors:

Arjen Weller, PhD Student

Jannik Larsen, Assistant Professor

Andrew Urquhart, Associate Professor

Poul Martin Bendix, Associate Professor

Technical University of Denmark
Department of Health Tech (DTU)
Colloids and Biological Interfaces (CBIO) group
Produktionstorvet, building 423,
2800 Kongens Lyngby, Denmark
s190671@student.dtu.dk

University of Copenhagen (UCPH)
Niels Bohr institute
Experimental Biophysics Research Group
Blegdamsvej 17, 2100 Copenhagen, Denmark
lwf546@alumni.ku.dk

Phone +45 61716241

Preface

This thesis is the result of a master's degree project (60 ECTS) at the Nanoscience center at the University of Copenhagen, Denmark. The master was written between February 2020 and August 2021, under the supervision of Professor Jannik Larsen at the Colloids and Biological Interfaces (CBIO) group at the Technical University of Denmark with Poul Martin Bendix as supervisor from the University of Copenhagen. The project was disrupted by the corona lockdown between March 2020 and May 2020.

This project aimed to elucidate the influence of double lipidation on internalization and transport of salmon calcitonin in the emerging Organ-on-a-chip system using fluorescent microscopy.

Date:

13.08.2021

Signature:

Emilie Kok, LWF546

Acknowledgement

Thanks to Jannik Larsen, Andrew Urquhart, and Poul Martin Bendix for making this project possible. Thanks to all the people of the CBIO group at DTU Health Tech for welcoming me and creating a comfortable working environment.
A special thanks to Arjen Weller for the training in cell culture, handling of the Organoplate®, introduction to the spinning disk confocal microscope, and etc. Thanks for keeping me on track and always answering my questions, when confusion struck. Thanks to Rodolphe Marie for letting me borrow the wide-field microscopy and to Adam Hundahl for helping me with the microscope and "holding my hand" during experiments.
A great thanks to Casper Hempel and all the people who were part of the project meetings, giving advice, inspiring talks, and support during the project.

I would like to thanks my family and friends for always encouraging me during my entire education, supporting me in tough times, and their continuous attempts to understand what I'm working with.
Thanks to Madklubben: Daniel, Emma, Lasse, and Sophie, for all the fun times, food, drinks, and company. Especially thanks to Daniel, my amazing partner, for supporting me and being the "housewife" for the last couple of weeks.

Abstract

Oral drug delivery has proven a favorable method of administrating drugs due to high patient compliance. Peptide drugs possess many advantages, such as high bioactivity and specificity. However oral drug delivery of peptide drugs is challenging owing to the biological barriers and acidic environment associated with the gastrointestinal tract. Lipidation of peptide drugs with lipid chains has proven to offer several benefits within oral drug delivery. This includes prolonged systemic circulation, increased enzymatic stability and lipid cell membrane interaction.

This study aims to investigate peptide transport across the intestinal barrier. The study is carried out using the therapeutic peptide salmon calcitonin (sCal), which lowers calcium in the blood. The study seeks to elucidate the influence of double lipidation on intestinal cell internalization and transport. The lipid chain length at position glutamine$_{20}$ and asparagine$_{26}$ is increased systematically. The use of the new emerging organ-o-chip-system allows tracking of peptides using live-cell imaging. Through the study, lipid length dependency on the internalization by the cells is revealed. Additionally, long-chain lipidation demonstrates accumulation beneath the cells. Recording the transport of the peptide analogs from one side of the cellular barrier to the other, reveal no transport at low concentration. Increased concentration of the peptide analogs, with non or short lipid chains, exhibit transport without any significant dependency on lipidation.

Resumé

Oral lægemiddellevering har vist sig at være en gunstig metode til administration af lægemidler på grund af en høj patientoverholdelse. Peptidlægemidler har mange fordele, såsom høj bioaktivitet og specificitet. Imidlertid er oral lægemiddellevering af peptidlægemidler udfordrende på grund af de biologiske barrierer og det sure miljø forbundet med mave-tarmkanalen. Lipidering af peptidlægemidler med lipidkæder har vist sig at have flere fordele inden for oral lægemiddellevering. Dette inkluderer forlænget systemisk cirkulation, øget enzymatisk stabilitet og lipid cellemembran interaktion.
Dette projekt har til formål at undersøge peptidtransport over tarmbarrieren. Projektet udføres ved hjælp af det terapeutiske peptid salmon calcitonin (sCal), som sænker calcium i blodet. Projektet søger at belyse indflydelsen af dobbelt lipidering på tarmcellens internalisering og transport. Lipidkædelængden ved position glutamin $_{20}$ og asparagin$_{26}$ øges systematisk. Brugen af det nye organ-on-a-chip-system tillader sporing af peptider ved hjælp af mikroskopi af levende celler. Gennem projektet demonstreres lipidlængdeafhængighed af cellernes internalisering. Derudover demonstrerer langkædet lipidation akkumulering under cellerne. Måling af transporten af peptidanalogerne fra den ene side af den cellulære barriere til den anden afslører ingen transport ved lav koncentration. Øget koncentration af peptidanalogerne med ingen eller korte lipidkæder udviser transport uden nogen væsentlig afhængighed af lipidation.

List of abbreviations

BCS	Biopharmaceutical classification system
BI	Barrier integrity
BSA	Bovine serum albumin
Caco-2 cells	Human colon adenocarcinoma cells
Cal	Calcitonin
CPP	Cell penetrating peptide
ECM	Extracellular matrix
FBS	Fetal bocine serum
GI tract	Gastrointestinal tract
Hbss	Hanks's balanced salt solution
hCal	Human calcitonin
LogP	n-octanol-water partition coefficient
MEME	Minimum essential medium eagle
NEAA	Nonessential amino acids
PBS	Phosphate-buffered saline
PE	Permeation enhancer
P/S	Penicillin-stretomycin
PSA	Polar surface area
Ro5	rule of 5
ROI	Region of interest
sCal	Salmon calcitonin
SDCM	Spinning disc confocal microscopy
TD	TRITC-dextran
TEER	Transepithelial/transendothelial electrical resistance
WFM	Wide-field microscopy

Contents

1 Introduction

Through the past years, designing an effective method of drug delivery has been of great interest.[1] Typical concerns related to injections are medication adherence of daily injections, an aversion to injections, worry about needle size, and discomfort of injections site.[2–4] By taking advantage of oral drug delivery these challenges can be avoided and high patient compliance along with ease of use can be achieved.[1,5,6] Since insulin therapy emerged in the 1920s, peptides have been widely used in medical practice.[7] Peptides are able to effectively disrupt protein-protein interactions and may serve as ligands for receptors of the cell surface[8] Oral peptide delivery is though facing other challenges. One of the greatest hindrances is the ability of peptides to pass through biochemical and physical barriers present in the gastrointestinal tract, resulting in bioavailabilities below a few percent.[6,7,9,10] Several different approaches to overcome these challenges have been developed, including permeation enhancers, cell-penetrating peptides, and lipidation of the peptide. However, each of these strategies has their limitations despite showing great potentials.[2,11,12]

Model systems to investigate the quality of potential new peptide drugs varies in a wide range of technical and biological complexities.[13] Standard *in vitro* systems usually include a static culture of epithelial cells on a rigid membrane. While the method provides quantification of peptide transport across the biological barrier, the method does not recapitulate the 3D cell organization and often no information is gained on the cellular mechanism.[14] The emerging field of Organ-on-a-chip technology present a potential alternative to the standard *in vitro* systems and animals models.[15] The Organ-on-a-chip system allows 3D cell organization, which has proven important for increased physiological relevance. Additionally, the system enables live-cell tracking using fluorescent microscopy.[16,17]

1.1 Aim of project

In this project, the influence of double lipidation on the internalization and transport of salmon calcitonin (sCal) is investigated. By these alterations, increased hydrophobicity and amphiphilicity are achieved while still preserving the cationic charge.[18] Salmon calcitonin (sCal) shares 50% amino acid identity with human calcitonin (hCal).[2] Hu-

man calcitonin, which is produced in the thyroid gland and secreted in response to an excess of calcium in serum, is physically and chemically unstable. However, sCal is more stable, potent, and has a longer in vivo half-life. Using single lipidated sCal analogs has proven both increased enzymatic stability and interaction with lipid cell membranes, along with prolonging systemic circulation time.[12] The internalization and transport of these double lipidated sCal analogs are investigated using human colon adenocarcinoma cells (Caco-2 cells) grown in an organ-on-a-chip system. The Caco-2 (human colon adenocarcinoma) model is used specifically for peptides and serves as the main method of investigating the permeability mechanism.[7] Caco-2 cells differentiate to form monolayers that resemble the small intestinal epithelium, both structurally and functionally.[19] Monitoring the internalization and transport of the sCal analogs are carried out using fluorescent microscopy.

2 Theory

2.1 Barriers to oral drug delivery

Understanding the gastrointestinal tract (GI tract) and sites of drug targets gives the opportunity to improve targeted oral delivery of peptides and proteins. There are several barriers to oral drug delivery including enzymes encountered through the GI tract, the mucosal barrier, and the physical barrier formed by the epithelial cells.[13] In the following part each barrier will be described in detail.

2.1.1 Gastrointestinal (GI) tract

The enzymatic degradation of orally administered drugs takes place all the way through the GI tract.[2,21] The function of the GI tract is to digest carbohydrates, proteins and other nutrients into amino acids and simple sugars. Additionally, the GI tract prevents then entry of pathogens.[22] This causes the oral bioavailability of intact peptides and proteins to be less than 1%, sometimes even less than 0.1%.[20] Through the GI tract two major biochemical barriers exist for orally administered peptides: enzymatic and pH. Through the GI tract, the oral administered peptides encounters several different proteases and other enzymes. The digestion first starts in the mouth, which is slightly acidic (pH: 6.5) and is rich on amylases and lysozymes.[2] However, since the residence and exposure time is minimal the buccal cavity is not considered a prominent barrier to oral drug delivery.[20]

The stomach and intestines presents the most active biochemical barriers to oral administered peptide's bioavailability. The production of gastric juice, composed of hydrochloric acid and mucus, causes the stomach to be an acidic environment (pH:1-2), which activates the proteolytic enzyme pepsin that acts as a endopeptidase, breaking proteins and peptides into amino acid, dipeptides, and tripeptides.[13] The digestion continues in the small intestines and due to increased pH in the small intestines the activity of pepsin stops. The small intestine is filled with other digestive enzymes, such as trypsins, chymotrypsins, exopeptidases and elastase.[23] As seen in figure 1 the small intestines consist of three main parts, duodenum, jejunum, and ileum. The oral administered peptide is subjected to a luminal pH that increases from the stomach (pH: 1-4) through the duodenum (ph:4-5.5), jejunum (pH:5.5-7) and ileum (pH:7-7.5). The increasing pH and varying

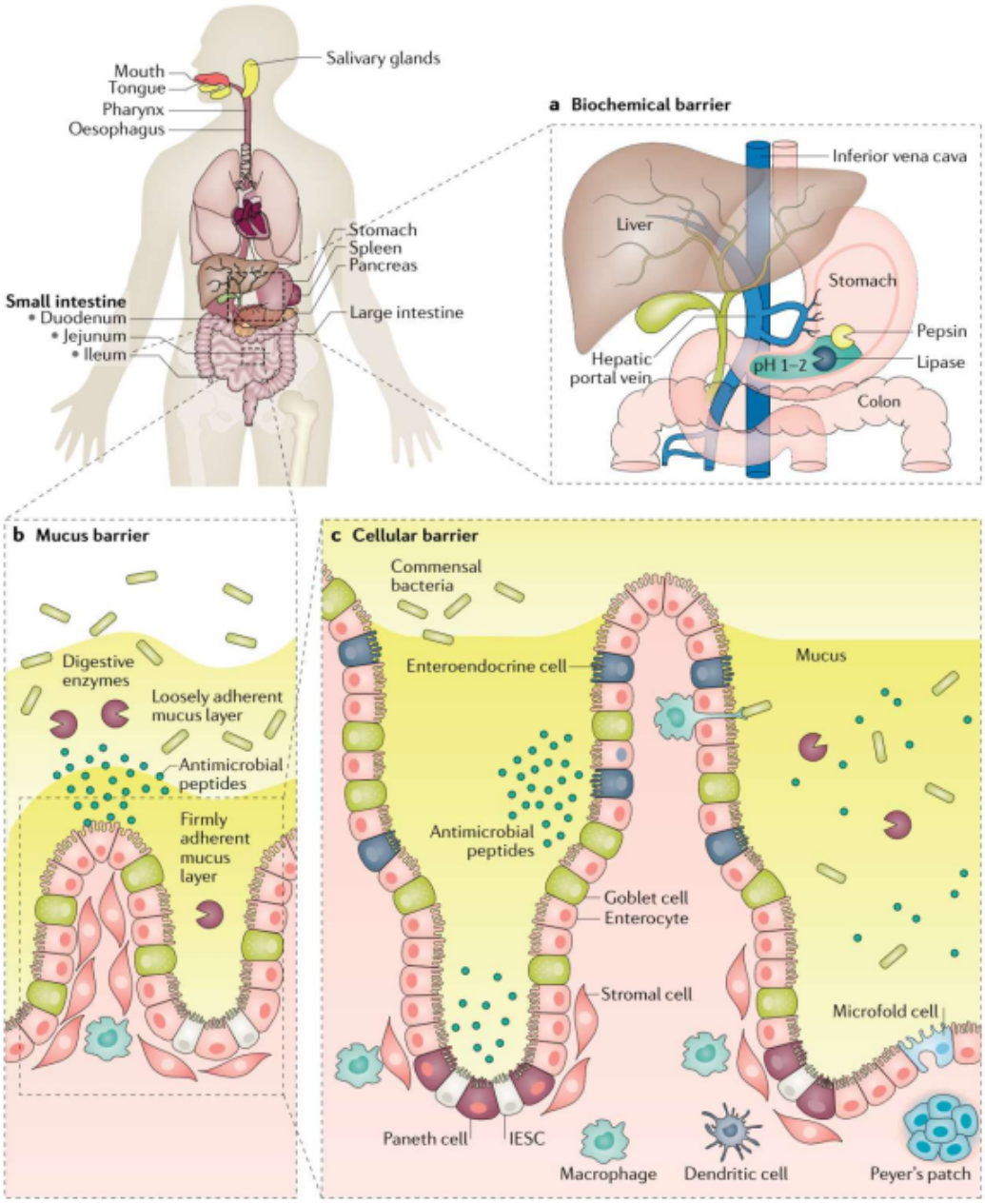

Figure 1: Multiple biological barriers protect the interior of our bodies against potential pathogens. The same barriers can also reduce the efficiency of oral drug delivery. **a**: Most proteins and peptides are stable around neutral pH. Upon entering the gastrointestinal tract the pH decreases drastically to pH 1-2 and encounters several proteolytic enzymes. **b**: The entire gastrointestinal tract is coated with a layer of mucus, which creates a physical barrier. Mucus is composed of mucin proteins, which by electrostatic forces traps molecules and contains proteolytic enzymes. **c**: The gastrointestinal epithelium comprises several different cells types and forms a barrier that regulates the transport of nutrients and proteins. Reproduction from Brown et al.[20]

gastric emptying have a strong influence of the pharmacokinetics of orally administered peptides. Protection from these enzymatic and pH changes are essential for effective oral peptide delivery.[24]

2.1.2 Mucosal barrier

Mucus is a viscoelastic, hydrogel-like structure lining the GI tract and is secreted by goblet cells. Mucus is mainly composed of mucins, which are heavily glycosylated glycoproteins with a tendency to form gels. Mucus also consists of water, lipids, electrolytes, immunoglobulins, antimicrobial peptides, protease inhibitors and various other proteins.[20] The mucus barrier is formed by a dense network of mucin fibers which consist of highly negatively charged segments with periodic hydrophobic domains. This forms strong electrostatic interactions and together with the viscoelasticity, the mucus layer exhibits protective properties toward particle diffusion.[25,26] The role of the mucus layer is to act as a lubricant for the passage of chyme, to protect the epithelium from damage, and to bind pathogens and foreign particles and hinder that they reach the epithelial cells.[13,27,28]

The GI tract is lined by two mucus layers: a loosely adherent layer and a firmly adherent layer as seen in figure 1. The firmly adherent layer is located immediately adjacent to the epithelial lining and includes cell-bound mucins as well as the glycocalyx.[20] The glycocalyx is a weakly acidic fuzzy coat that covers the top of the epithelial cells. The glycocalyx consists of bicarbonate ions secreted from the epithelial cells.[26] As the mucus layer, the glycocalyx also presents a protective barrier. The glycocalyx restricts the direct contact of microorganisms and particles with the epithelial cells.[13] The loosly adherent mucus layer undergoes constant turnover, which contributes the the elimination of pathogens. The particles retention at the mucus surface is influenced by the interactions between the particle and mucus and the low permeability is currently one of the biggest challenges to orally administrated drugs. Managing to diffuse through the mucus layer, leads the particle to the epithelial surface.[25,26]

2.1.3 Epithelial lining

The intestinal lumen is a single layer of cells organized in a finger-like structure, known as the epithelium, forming crypts and villi as seen in figure 2. The finger-like structure

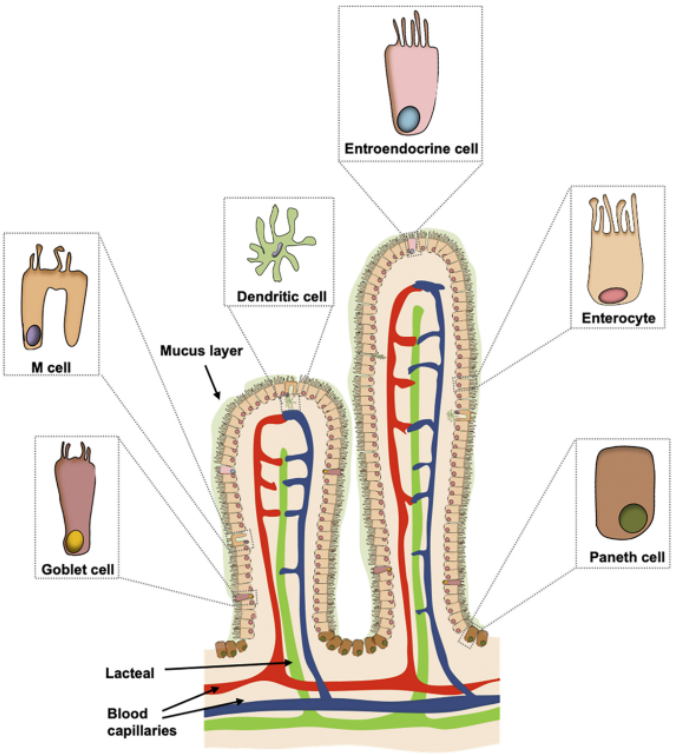

Figure 2: Schematic representation of the various cells types present in the intestinal epithelium. Reproduced from Xu et al.[28]

increases the internal surface area of the small intestines and is, therefore, the major place for absorption of food.[7,29] The epithelium is anchored to an underlying tissue via a basal lamina. This side of the cells is known as the basal side, while the opposite side is known as the apical side. The apical side is covered by a mucosal layer and exposed to the lumen of the intestines. This means that the epithelium is structurally polarized, as the individual cells it consist of.[30] The function of the intestinal epithelium is to serve as a selective permeability barrier. The epithelium separates the fluid from the basal side from the fluid with a different chemical composition on the apical side. This barrier function requires the adjacent cells to be sealed together, by what is called tight junctions, that prevent the molecules to freely leak through the cell sheet.[20]

Dividing cells are restricted to the crypts, while differentiated cells, with a sliding movement, travel upwards to the top of the villi, where they undergo apoptosis and are discarded into the lumen of the gut.[30] The epithelium consists of different types of cells, the majority being enterocytes as can be seen in figure 2. Enterocytes are polarized columnar epithelial cells. The apical side is covered with a closely packed microvilli brush border and a carbohydrate glycocalyx. The mucus secreting goblet cells are the second most

commonly found cells in the small intestines. The secreted mucin forms the protective layer that covers and protects the epithelia. Even though the epithelia consist of less than 1% of M cells, these cells play an important role in the uptake of antigens and microorganisms. Dendritic cells are responsible for maintaining immune environment homeostasis in the intestine. Paneth cells are located at the base of the crypts and are a part of the innate immune defense system, by secretion of antimicrobial proteins and peptides. Although low in number, the epithelia also contains enteroendocrine cells, interspersed among the other epithelial cells. Enteroendocrine cells consist of more than 15 different subtypes. They secrete serotonin and peptide hormones that are involved in the growth regulation, proliferation, and digestive activities of cells in the gut. The epithelium has a highly conserved morphology and contains many different cell types each performing distinct functions keeping the barrier homeostasis.[28]

2.1.3.1 Tight junctions

The last barrier orally administered drugs have to pass is the cell lining of the epithelial membrane. Passage of molecules between adjacent intestinal cells is restricted by tight junctions, adherens junctions, and desmosomes.[20] Together these three junctions comprise the apical junctional complex seen in figure 3, which encircle the epithelial cells and ensures the epithelial structure and integrity. Desmosomes and adherens junctions contribute to the adhesive force that is necessary to maintain the interaction between adjacent cells. Cadherins, the most well-known component of the adherens junction, are single-spanning transmembrane proteins that interact identically with the extracellular part of cadherins on adjacent cells. The cytoplasmic portion of cadherins interact with p120-catenin and β-catenin, which then interact with α-catenin.[31] The tight junctions form branching strands that are composed of rows of transmembrane proteins, predominantly the claudins family and occludin, with their extracellular domains forming loops that bind to corresponding loops of adjacent cells. The extracellular domain of claudins on adjacent cells forms pores that are responsible for the regulation of the tight junction ion selectivity.[13] The peripheral scaffold protein zonula occludens (ZO1, ZO2, and ZO3) interacts directly with the transmembrane tight junction proteins, including claudins, and the tight junction-associated MARVEL protein family, including occludin. The ZO proteins also connect to the cytoskeleton components, such as actin and myosin, via linker

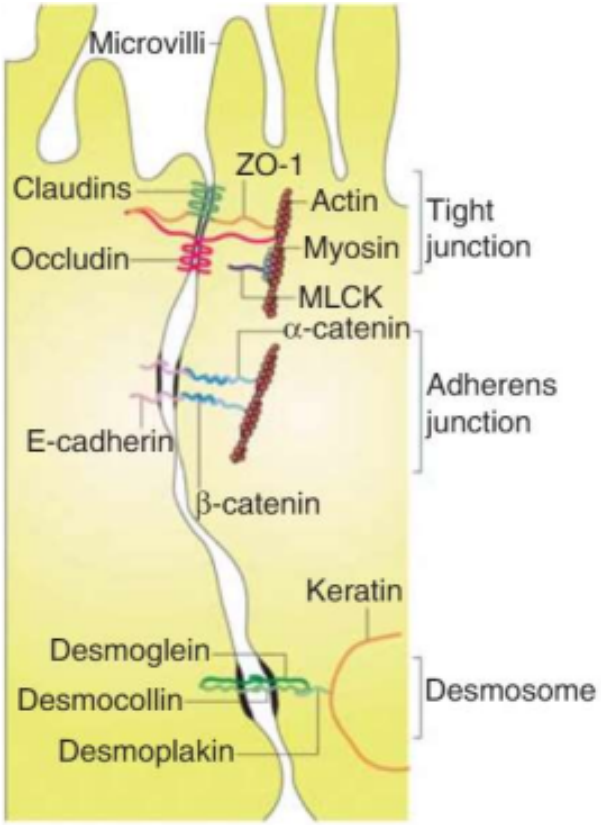

Figure 3: Schematic of the apical junctional complex of an intestinal epithelial cell. Claudins, ZO-1 and occludins form the tight junctions, while E-cadherin, α-catenin and β-catenin interact to form the adherens junction. Desmoglein, desmocollin, desmoplakin and keratin filaments interact to form desmosomes. Reproduced from Buckley et al. [32]

proteins. [31]

2.2 Transport mechanism through the GI tract

In the following section the different transport mechanism across the epithelial layer will be discussed. The passage of orally ingested peptide drugs can either be achieved through the paracellular route, which involves the intercellular space surrounding and between the cells, or the transcellular route, which is transit through the cells. [2] In figure 4 an illustration of the transport mechanism can be seen.

2.2.1 Paracellular permeability pathways

Transport of molecules through the tight junctions of two adjacent cells across the epithelial cells is termed *paracellular transport*. The tight junctions provides both charge

and size selectivity, while two distinct routes, termed the *pore* and *leak* pathway, exist.[31] These pores constitute approximately 0.01-0.1% of the total intestinal epithelial surface area, which is $\sim 32m^2$,[7] which causes the route to be preferred by low molecular weight hydrophilic compounds, such as peptide and protein molecules which naturally have logP value < 0.[6] The penetration ability of polar molecules is limited by the tight junctions between the epithelial cells in the GI tract and depends on their molecular dimensions and ionic charge. A molecular weight beyond 700 Da decreases the bioavailability rapidly. This is unfortunate since most therapeutic peptides and proteins have molecular weights far greater than 700 Da, which causes them to have low bioavailability. Hence this pathway is not an ideal option for transport most therapeutic peptides and proteins.[6,10]

2.2.2 Transcellular pathway

Passive transcellular diffusion is the main pathway for many small-molecule drugs that have good membrane permeability. Transcellular transport requires passive diffusion through the apical membrane, facing the gastrointestinal tract, into the enterocytes, followed by diffusion across the cell and through the basolateral membrane into the blood.[33] The surface area of the intestinal epithelial layer is approximately 32 m^2 in humans, providing a massive input of the drug into the system in all cases where the permeability is not dependent on transporters.[7] This route is ideal for small-molecules, but physicochemical properties, such as molecular weight, charge, lipophilicity, and polar surface area (PSA), play an important role.[6] The lipophilicity of a molecule is one of the most important factors that influences the transport via the transcellular pathway since it has to pass the lipid bilayer of the intestinal membrane. This causes significant challenges in the transport of proteins and peptides through the transcellular pathway.[10] These properties affecting this pathway will be discussed in the following section.

2.3 Improvement of peptide drug delivery

For decades, small molecule drugs have been dominating the pharmaceutical industry. In 1997 the guideline, known as the 'rule of 5' (Ro5), was developed by Lipinski et al. to predict and reduce the risk of inadequate oral absorption due to poor solubility or poor permeability of small molecules.[35] These guidelines favor small molecules with fewer than 5 hydrogen bond donors, fewer than 10 hydrogen bond acceptors, molecular weight

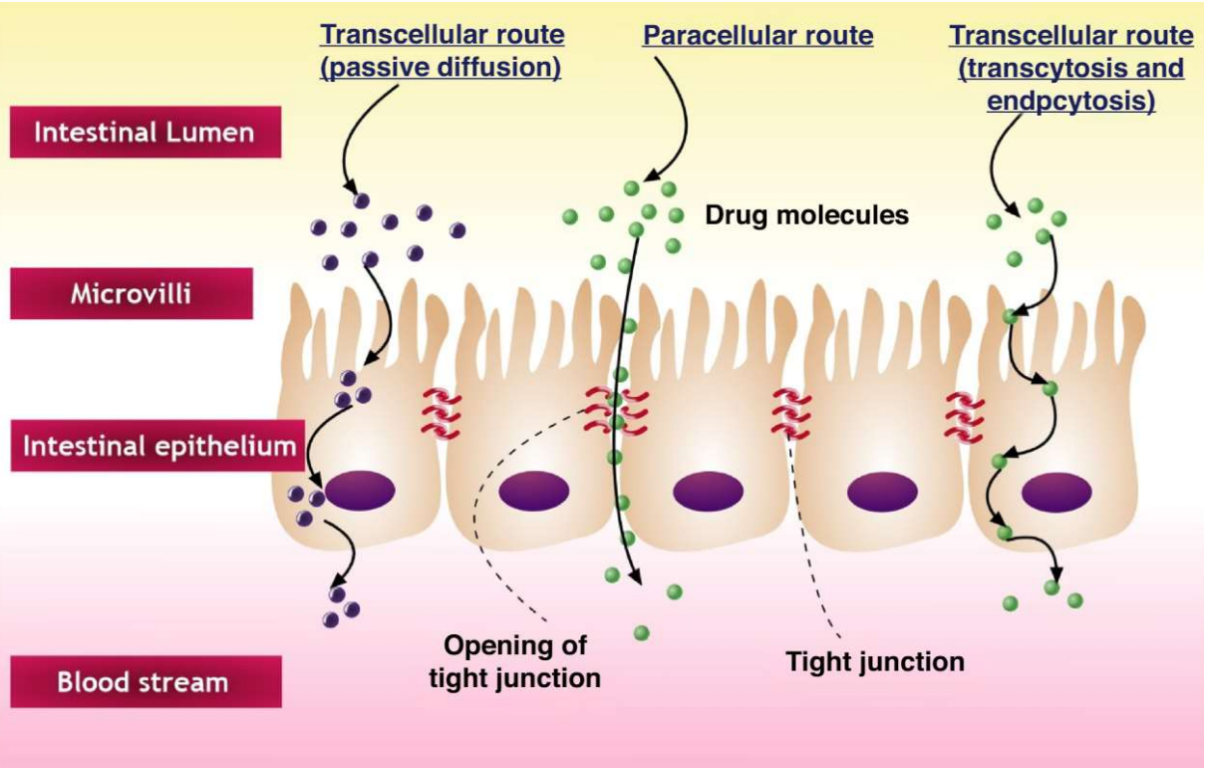

Figure 4: Transport mechanism of protein and peptide absorption. Smaller peptides are taken up by the paracellular pathway, while larger peptides with adequate lipophilicity exploit the transcellular pathway. Reproduced from Dubey et al.[34]

less than 500 Da, and an n-octanol-water partition coefficient logP, which is a method of evaluating the lipophilicity, no greater than 5. According to the Ro5, 90% of oral compounds pass three of four of the aforementioned rules.[8] Even though the Ro5 has reduced attrition due to poor pharmacokinetics, doubt has emerged if whether this may have resulted in lost opportunities.

A great interest has been put in drug molecular entities based on peptides and proteins as therapeutics due to their potency and specific mode of action, which results in predictive response and fewer side-effects when comparing to conventional small molecule synthetic drugs.[5] The Ro5 has also been applied to peptide drugs, though the 500 Da molecular weight threshold is reached with only 5 amino acids and therefore is not compatible with the determination of peptide bioavailability. A different rule set specific for peptides has been suggested by Veber et al. For the prediction of good bioavailability of peptides. Only two criteria are necessary: a PSA below 140 Å and 10 or fewer rotatable bonds.[7]

2.3.1 Why oral drug delivery

Currently, these protein and peptide drugs are mainly administered via injection, which can be associated with pain and discomfort by the patient.[2] Instead, drugs administered orally are widely accepted by patients. Since there is no need for sterile manufacturing, cold storage, or assistance from health care personnel, as with injectable formulations, the cost associated with production, storage, and use of oral dosage formulations is usually lower. The quality of life for millions of people suffering from chronic diseases which require frequent injections, such as diabetes and osteoporosis, would inevitably increase with oral dosage forms as substitutes to injectable drugs.[5,6,33] An extensive research done by Doak et al. confirms that oral drugs are found far beyond the Ro5. Increased reliability of exposure, ability to deliver large variations in dosage and potentially greater storage stability are some of the advantages oral delivery posses compared to other noninvasive delivery methods, such as buccal, nasal, and transdermal, when systemic exposure of a drug is wanted.[33] Though it is important to consider both the physicochemical properties, such as molecular weight, size, and hydrophobicity, and the biological barriers that restrict the absorption in the GI tract, when developing peptides for oral drug delivery[6,9,10]

2.3.2 Physicochemical factors that affect oral bioavailability

Lipophilicity of a molecule refers to its ability to readily dissolve in lipid, oil, or nonpolar solvent. Drugs are classified into four groups, I) high solubility and high permeability II) low solubility and high permeability III) high solubility and low permeability IV) low solubility and low permeability, by the biopharmaceutical classification system (BCS), according to US FDA.[34] Peptide drugs often belong to BCS III or even BCS IV and when administered orally the chemical structure exposes fundamental drawbacks due to relatively high molecular weight and high hydrophilicity, which limits their ability of absorption in the GI tract.[36] The logarithmic ratio of the partition coefficient (logP) allows evaluation of the lipophilicity of a drug.[7]

Molecular size/Molecular charge of orally administered peptide drugs have a huge influence on the bioavailability of the drug. The structure of the epithelial cells in the GI tract allows small molecules to passively transport through the cell monolayer, while

the larger molecule's potential energy is too low to allow this form of transport. Although small molecules of 75-100 Da are able to pass through the epithelial layer, the smallest peptides are 700 Da. The size of an orally administered drug is, therefore, a crucial limiting factor of bioavailability.[34,36] Replacing a single nonpolar amino acid, in a peptide drug, with a polar amino acid results in a strong decrease in permeability. This has been shown in previous studies where the nonpolar amino acid Alanine was replaced with either the negatively charged amino acid Aspartate or the positively charged amino acid Arginine.[7]

Polar surface area (PSA) are one of the additional descriptions for the prediction of oral bioavailability. PSA is the amount of the surface area of the polar atoms, such as nitrogen and oxygen, in macromolecules. Oral administered drugs with a PSA greater than 140 $Å^2$ are supposed to exhibit a low epithelial cell membrane permeability.[36] Though there are some FDA approved drugs that have PSA $>$ 140 $Å^2$, some even as high as 200 $Å^2$.[37]

2.3.3 Overcoming the barriers in oral peptide drug delivery

Permeation enhancers (PE) alters the structure of the cellular membrane which influences the transcellular route and/or the tight junctions between adjacent cells (paracellular route) of the intestinal epithelium.[10,36,38] PEs which increase the permeability in different *in vitro* models, including across Caco-2 monolayers, may improve oral bioavailability, but not guaranteed. Previous studies have shown that the enhancer efficacy is often accompanied by toxicity which has limited the use of PEs in oral formulations. The potential of using PEs for oral drug delivery is though still not clarified since it is unclear if the experimentally observed correlation between the potency and toxicity of PEs is a consequence of limited conditions in the studies.[38]

Cell penetrating peptide (CPP) studies have in recent years demonstrated the potential of these peptides to facilitate the permeation of peptide drugs across the intestinal epithelium.[39] The present CPPs show great variance in the primary sequence as well as their secondary structure, though they still share some common features. CPPs are generally short peptide sequences of less than 30 amino acids and they are typically rich

in arginine and lysine residues. These residues enable electrostatic interactions with the negatively charged molecules present on the cell surface.[13,36] Additionally positive influence on the translocation of the CPP is achieved by the presence of hydrophobic amino acid residue such as tryptophan.[29]

Lipidation of therapeutic peptides with fatty acids is a well-known strategy used in peptide oral drug delivery. Lipidation of peptides changes the hydrophilicity and the secondary structure, which may enhance membrane penetration, prolonging the peptide circulation in the blood and increases the enzymatic stability.[36,40] Lipidation may influence some of the current challenges of oral drug delivery, since it is a promising method to protect the peptides against enzymatic degradation, thereby making the peptides more lipophilic which results in increased permeability.[6,11] This method has been used for several therapeutic peptides, including marketed drugs like insulin and Glucagon-like peptide-1.[12]

2.4 Salmon Calcitonin (sCal)

Calcitonin (Cal) is a 32 amino acid single-chain peptide hormone secreted by the cells of the thyroid gland. Cal has a disulfide bridge between positions 1 and 7 in the N-terminal and a C-terminal amidated proline.[12] Cal is secreted in response to excess calcium in the serum and plays a crucial role in both calcium homeostasis and bone remodeling. The primary biological function is the inhibition of osteoclast-mediated bone resorption. This has caused calcitonin to be used as a treatment of bone-related disorders, such as osteoporosis, osteoarthritis, Paget's disease, and hypercalcemia. However, a frequent and relatively high dosage of Cal through injections is necessary.[41] Even though this is a fast and easy way of administering the peptide drug, it leads to problems with patient comfort and compliance, which have encouraged the search for alternative delivery ways, including oral delivery.[42] However Cal shows extensive proteolytic degradation in the GI tract, intrinsic intestinal membrane permeability and insufficient oral bioavailability.[41] Synthetic and recombinant calcitonin has been derived from several other species.[41] Salmon calcitonin (sCal), which shares 50% amino acid identity with human calcitonin (hCal), is the most widely used since it is more stable, have longer *in vivo* half-life[12] and 50-100 times more potent than hCal,[43] though its bioavailability is still less than

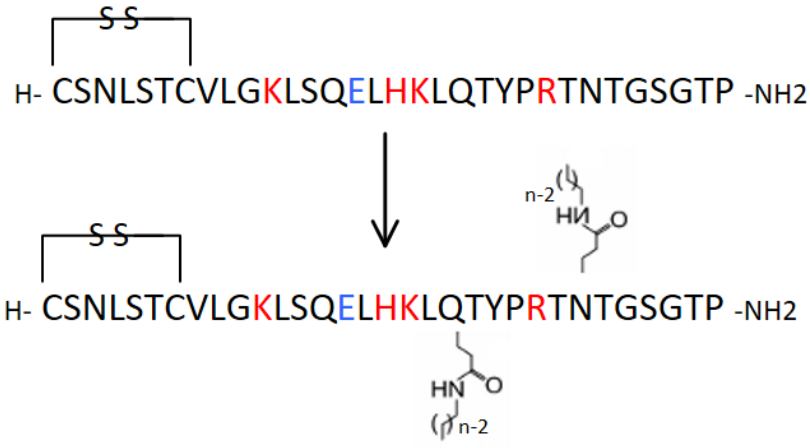

Figure 5: Schematic representation of the sCal analogs. **Top.** sCal with basic (red) amino acids highlighted. **Bottom.** sCal is shown with basic (red) and acidic (blue) amino acids highlighted. The lipidations are indicated at the glutamine$_{20}$ and asparagine$_{26}$ position, with varying lengths (n) equal to either C4, C8, C12 and C16.

1-2 %.[41] Therefore the need of alteration of the peptide is crucial.

As discussed in the previous section about physiochemical factors influencing oral bioavailability and how to overcome the barriers of oral peptide delivery, several factors are important and different approaches are available. Inspired by the work done by Trier et al.[12] this project takes advantage of acylated sCal analogs. A series of analogs of the therapeutic peptide sCal have been synthesized. Saturated chains of variable lengths, C4, C8, C12, and C16, have been introduced at the glutamine$_{20}$ and asparagine$_{26}$ position in the peptide sequence. A schematic of the amino acid sequence and alteration can be seen in figure 5. Viewed from the endpoint, the peptide form a helix with the positive and negative amino acids on each side which can be seen in the helical wheel in figure 6. Through this approach, the hydrophobicity and amphiphilicity of the peptides are increased while the cationic charge is preserved. This causes the peptide to be similar to cationic cell-penetrating peptides.[18] The transport and uptake of these peptide analogs will be investigated in a newly emerging system, referred to as organ-on-a-chip, which will be discussed in one of the following sections.

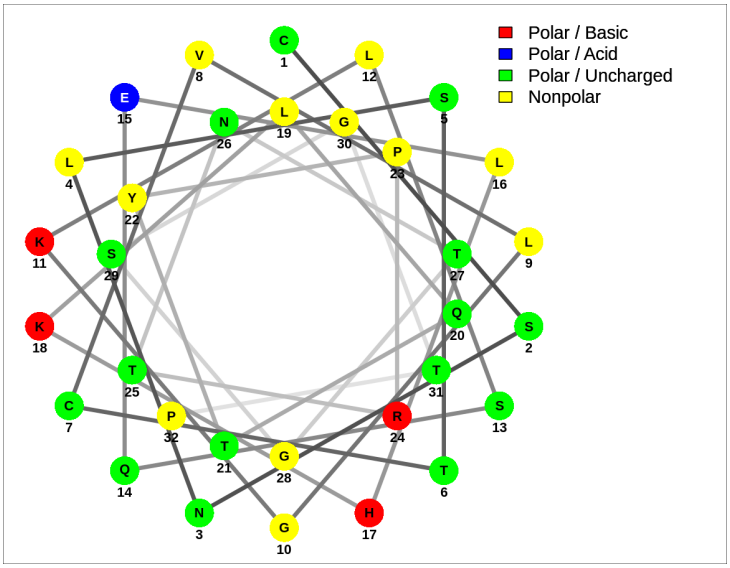

Figure 6: Helical wheel of sCal with basic (red) and acidic (blue) amino acids highlighted.

2.5 Caco-2 Cells

In the 1980s, due to difficulties in obtaining intestinal differentiated cells lines in culture from normal tissue, attention went to the specific intestinal properties of gastrointestinal tumoral cell lines, which were collected a decade earlier for cancer studies. One of these cell lines, the Caco-2, showed spontaneous differentiation, expressing several morphological and biochemical characteristics of small intestinal enterocytes.[44] These cells grow in monolayer and show polarized morphology, with microvilli on the apical side and tight junctions between adjacent cells. Other enterocytic characteristics of the Caco-2 cells are polarized membrane receptors of growth factors and transport activities on both membranes. To better reproduce the conditions existing in the intestines *in vivo*, Caco-2 cells were cultured on a permeable filter allowing free access of ions and nutrients to both sides of the monolayer. These conditions led to improved morphological and functional differentiation. Since then, they have been extensively utilized as a model for intestinal transport and toxicity assays.[19,44] The variation in culture protocols makes it often difficult to compare results. Several effects of cell and culture-related factors on the morphology and functionality of Caco-2 cells have to be considered. One of these factors is the number of passages (the age) in culture. The number of passages was first shown to influence the expression of typical differentiation markers of intestinal enterocytes, which increased with passages. Several others have since shown that increasing passage number influences different functions and activities of Caco-2 cells. This includes

an increase in proliferation rate and the appearance of multilayered areas.[44] In order to obtain reproducible experimental models and comparable results, culture-related factors have to be considered. Time of culture and seeding densities can influence cell replication, senescence, and differentiation. Since the differentiation process of cells only starts when cells reach confluence, the seeding density is an important factor related to differentiation traits. This means, seeding different densities leads to a variation in the differentiation stage related to the number of days in culture.[44] A study by Behrens and Kissel[45] showed that the seeding density influenced the monolayer structure and carrier-mediated transport, while no difference in paracellular permeability and TEER was observed. They found that using a seeding density of 6 x 10^4 cells/cm^2, on a permeable filter substrate, lead to good differentiation after three weeks in culture. This is comparable with the recommended seeding density by American Type Culture Collection is 4 x 10^4 cells/cm^2 in a T75 flask.[46] Behrens and Kissel[45] also found that higher seeding densities lead to the formation of multilayers. Caco-2 cells exhibit a higher activity of P-gp compared to the human intestine, which should be considered when using these cells as a model for intestinal bioavailability.[44]

2.6 Development of the 3D culture system

2.6.1 Going from 2D to 3D system

Testing potential therapeutics and modeling disease mechanisms have normally been carried out via the use of animal models or cell cultures. Animal models exhibit the natural complexity of multicellular, multi-organ, and multi-system interactions, which forms complex architecture that causes varying degrees of similarity between human pathophysiology and the animal model.[47] Traditionally drug development models, like animal testing, often fail to predict drug effects at the human clinical trial stage, which significantly increases the cost and patient risk. The time and cost of using animal models add to the concerns of use. The cost of developing one clinically applicable drug has increased from 800 million dollars to nearly 2.5 billion dollars today and takes around 10-15 years.[16,17,48] Furthermore the ethical concerns of using animal models also contribute to the limitations of their use as models of disease and screening platforms for potential therapeutics.[47] One of the most common 2D cell culture systems to study in-

testinal permeability is the Transwell®. The epithelial cells are seeded on a membrane on a "transwell insert". This insert separates the apical and basal compartments. The model is highly standardized and easy to used.[49] Conventional two-dimensional (2D) cells cultures fail to support the tissue-specific, differentiated functions of numerous cell types and lack the possibility to provide information regarding the complexity of living systems.[50,51]

Based on these drawbacks, the need for improvement of drug development models is clear. Over the past decade, microfluidic systems, known as organ-on-a-chip, have emerged as cost-effective high-throughput systems for *in vitro* modeling.[16] In contrast to animal models, these miniaturized tissue models enable direct access to cells within their architecture to probe their functional changes in response to drug stimulation in real-time.[17] The embedment of cells in an extracellular matrix leads to more relevant physiological behavior, such as apical-basal polarization, lumen formation, reduced proliferation, and increased differentiation.[52,53] By better recapitulate the physiological conditions a more accurate prediction of drug carriers' effect can be achieved, which provide a sophisticated *in vitro* screening model to fill the gap between animal models and human clinical trials.[54] However as a new and still emerging field, the lack of a standardized automated fabrication process gives rise to hurdles in terms of becoming easy to use, scalable, reproducible, and user-friendly systems.[51]

2.6.2 Organ-on-a-chip

The most common model of studying barrier function and drug absorption *in vitro*, uses culturing of human intestinal epithelial cell lines, such as Caco-2 or HT29-MTX, on extracellular matrix (ECM) - coated, porous membranes in Transwell culture devices. Even though the model is commonly used in the pharmaceutical industry, this 2-dimensional model does not recapitulate physiological 3-dimensional intestinal cells, tissue morphology, and other differentiated functions, such as mucus production and villi formation.[55] These challenges have been overcome by the development of the organ-on-a-chip system, where cells are cultured in engineered micrometer-sized chambers, constantly perfused with required nutrients. The ability to introduce constant fluid flow and the use of low cell numbers have proven to be beneficial since the cells polarize faster and have higher expression of specific proteins such as mucin.[16] The system geometry and structure of

the system mimics the physiological length scales and concentration gradients, while the fluid flow generates mechanical forces that imitate the *in vivo* microenvironment cells experience.[54] Most microfluidic intestine devices consist of 2 hollow channels separated by ECM-coated polyester or polycarbonate membrane, which have immortalized human epithelial cells cultured on one of its surfaces. The epithelial monolayer can access from both the apical and basal sides, which enables quantification of tight junction barrier function and absorption of nutrients and drugs.[55]

2.6.2.1 Organoplate®

One company that produces this organ-on-a-chip system is Mimetas, which has productized a multi-well plate called the Organoplate® which is based on a 384-well microtiter plate format containing 40 microfluidic chips, which each is positioned under 9 wells in a 3x3 grid. A single chip consists of three channels, a center channel, and 2 adjacent channels.[56,57] The Organoplate® utilizes a unique patented technology called Phaseguides™, which are meticulously designed meniscus pinning barriers. This technology allows the precise, barrier-free definition of culture matrices and cells in 3D. Additionally, cell-cell interactions are supported and unprecedented imaging and quantification are now possible.[14,17,58,59] As illustrated in figure 7 ECM are pipetted in the gel inlets where the Phaseguides™ act as capillary pressure barriers that directs the hydrogel through the chip. After gelation, cells are seeded in the adjacent channel, allowing them to sediment directly against the ECM gel by placing the plate in a vertical position. When attached, the plate is horizontally placed on an interval rocker that induces bi-directional gravitational flow.[17,48,57]

2.7 Microscopy

2.7.1 Widefield microscopy

Widefield microscopy is one of the most basic techniques within microscopy and is fundamentally a technique in which the entire sample is exposed to the light source. One type of widefield microscopy is brightfield, which illuminates the sample using white light. Standard widefield microscopes usually consist of a white and fluorescence light source. Usually, the excitation light in widefield microscopy has been arc lamps, commonly the mercury arc lamp and the xenon arc lamp. These lamps provide extremely intense light

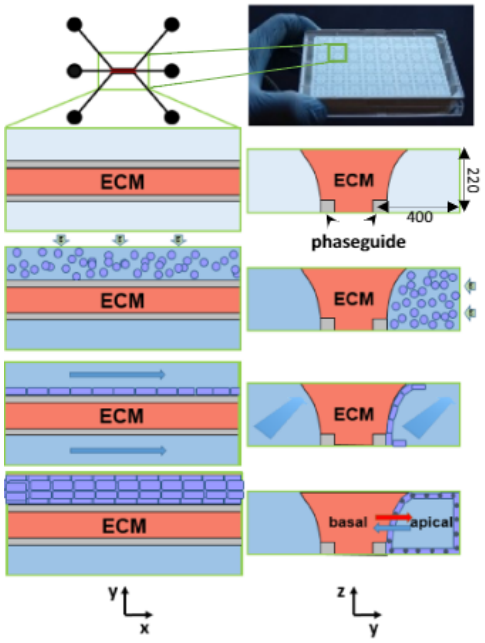

Figure 7: Seeding cells against ECM: After loading ECM into the middle channel, cells were seeded in the adjacent channel. By gravity, cells are triggered to attach to the gel. After inducing flow, cells start growing a perfused tubular structure. Dimensions of the channels are in micrometer. Reproduced from Vormann et al.[60]

sources, but the lifetime of these light sources is very limited to around 200-600 hours. Instead, a new generation of light sources, light-emitting diodes (LED), is introduced. These LEDs provide a high-intensity light source, which covers a full spectrum of excitation wavelengths (365 nm to 770 nm). Compared to the arc lamps, these LEDs have a lifetime of up to 50000 hours, which is a great advantage.[61]

2.7.2 Spinning disk confocal microscopy (SDCM)

Imaging thick fluorescent specimens, such as cells, can cause problems for conventional widefield microscopy. This is due to increased background signal and a low contrast image, which is because of fluorescent signals from objects outside the focal plane. Spinning disk confocal microscopy (SDCM) takes advantage of a multi-pinhole Nipkow spinning disk, which contains multiple sets of holes, arranged in a spiral. This causes the sample to be illuminated with thousands of laser beams simultaneously.[62] By keeping the sample placed along the light path ensures that the focus is kept at a fixed distance from the objective. By also incorporating a stepper motor for the z-axis and three-dimensional imaging software allows scanning of different fields of view through the specimen. This

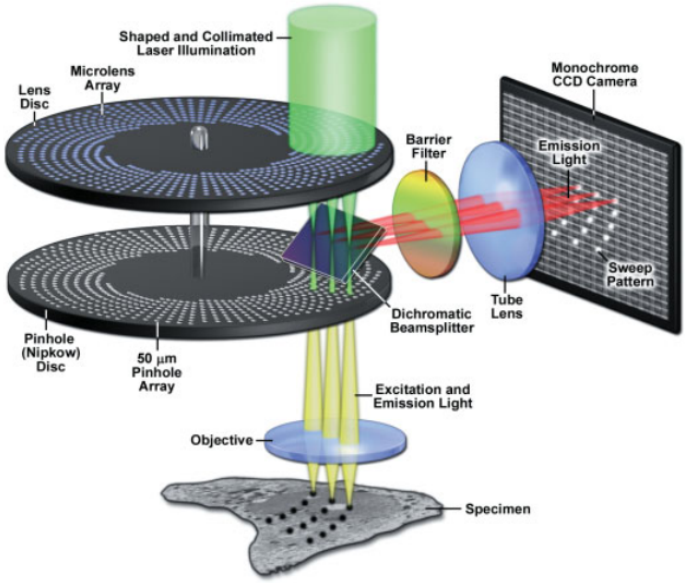

Figure 8: Setup of a spinning disk confocal microscopy, using a Nipkow disk. The setup contains two disk that rotate as a single unified piece. The upper disk focus the incident beam on a pinhole in the second the disk. The pinholes of the second disk are confocal with a specimen. Reproduced form Fundamentals of light microscopy [62]

makes it possible to collect a series of in-focus optical slices for 3-D reconstruction. [63,64] However, it is not until recently that the spinning disk system is used for fluorescent microscopy since it was not possible to transmit enough excitation light through the Nipkow disk to the sample. This caused an insufficient confocal signal. By introducing a dual disk containing microlenses, combined with high-intensity laser light and sensitive digital cameras, the problem was overcome by Yokogawa Electric Corporation. [65] The setup of the spinning disk system can be seen in figure 8. The technology of spinning disk yields a desirable low-cost imaging system. The spinning disk system has been widely used for situations, such as live-cell imaging, where long times imaging is necessary while still minimizing photon damage. [62]

3 Results

Through the rest of the project internalization, translocation and transport will be discussed. The three events is defined as followed.

- Internalization: uptake by the cells meaning transfer from the lumen of the Caco-2 tubule to inside the cells.
- Translocation: transfer from the lumen of the Caco-2 tubule, through the cells and down below the cells.
- Transport: transfer from the lumen of the Caco-2 tubule to the ECM.

3.1 LDH cytotoxicity assay revealing concentration dependency of peptides analogs with lipid length C8,C8, and longer.

Using a Pierce LDH cytotoxicity assay the cytotoxicity of a range of sCal analogs are studied. The cytotoxicity assay is performed at 680 nm (background) and 490 nm. To calculate the cytotoxicity the background signal is subtracted from the 490 nm signal. The signal from each peptide analog at each concentration is divided with the signal from the positive control and multiplied by 100. The means are calculated from each sample and can be seen in figure 9. A control without any peptide analog is also measured. At the y-axis the cytotoxicity % can be seen, while on the x-axis the different sCal analogs are indicated. The color scale corresponds to the different concentrations. Starting by looking at the sCal(C0,C0), very low cytotoxicity below 5% is seen for all the concentrations. The cytotoxicity is equal to what is seen for the control. The concentration does therefore not seem to have an impact on the cytotoxicity of this peptide analog. Comparing with the sCal(C4,C4), the cytotoxicity has a small increase, but at all concentrations, it is still less than 7%. The cytotoxicity is still constant in regards to increasing concentration. The lipidation with lipid lengths of 4 carbons does not seem to have an impact on the cytotoxicity of the sCal, though increasing the chain lengths further does. Looking at the sCal(C8,C8) and the sCal(C12,C12), the cytotoxicity increases drastically. Already at 5μM, the cytotoxicity is 10% and 20%, respectively. From there the cytotoxicity has most of the time a steep increase up to around 60% and 80%, respectively, at 75 μM. sCal(C8,C8) and sCal(C12,C12) clearly have a different trend,

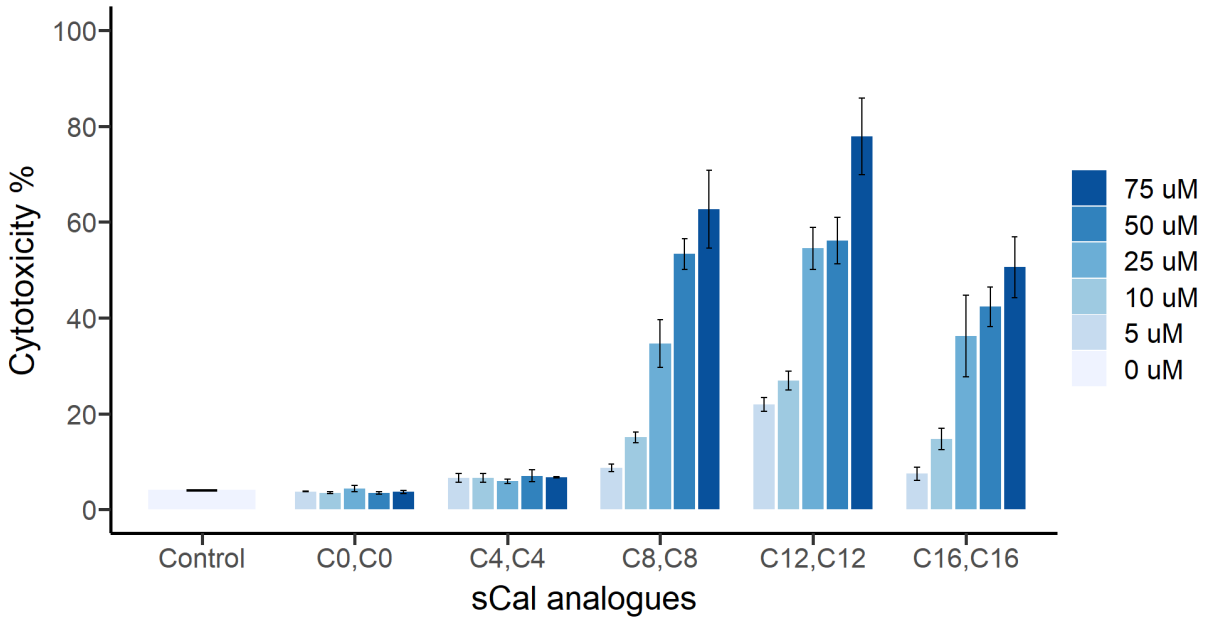

Figure 9: **LDH cytotoxicity assay revealing concentration dependency on cytotoxicity of peptides with chain length C8,C8 and longer.** Cytotoxicity of five sCal analogs measured using ad Piere LDH cytotoxicity assay. The errobars are calculated as standard error of the mean with n=3.

comparing to the sCal(C0,C0) and sCal(C4,C4), with the concentration having a great influence on the cytotoxicity. At this point, the lipid lengths show a clear influence on the cytotoxicity with a trend of increasing lipid length leads to increasing cytotoxicity. At lipid lengths equal to sCal(C16,C16) the concentration dependency shows the same trend as sCal(C8,C8) and sCal(C12,C12). However looking at the last sCal analog sCal(C16,C16), which has the cytotoxicity at each concentration is lower compared to sCal(C12,C12). Since sCal(C0,C0), sCal(C4,C4) and sCal(C8,C8) showed the lowest cytotoxicity, these peptide analogs are used forward.

3.2 Cell characterization confirms tight junction and brush border formation of Caco-2 tubules grown in organoplates.

3.2.1 Loading and seeding of chips

The human adenocarcinoma cell line (Caco-2 cells) is grown in a T75 flask. When reaching confluency, they are trypsinized and cell solutions of 1 x 10^7 cells/mL are prepared. 2μL of cell solution is injected into the media inlet of the Organoplate® which can be seen in

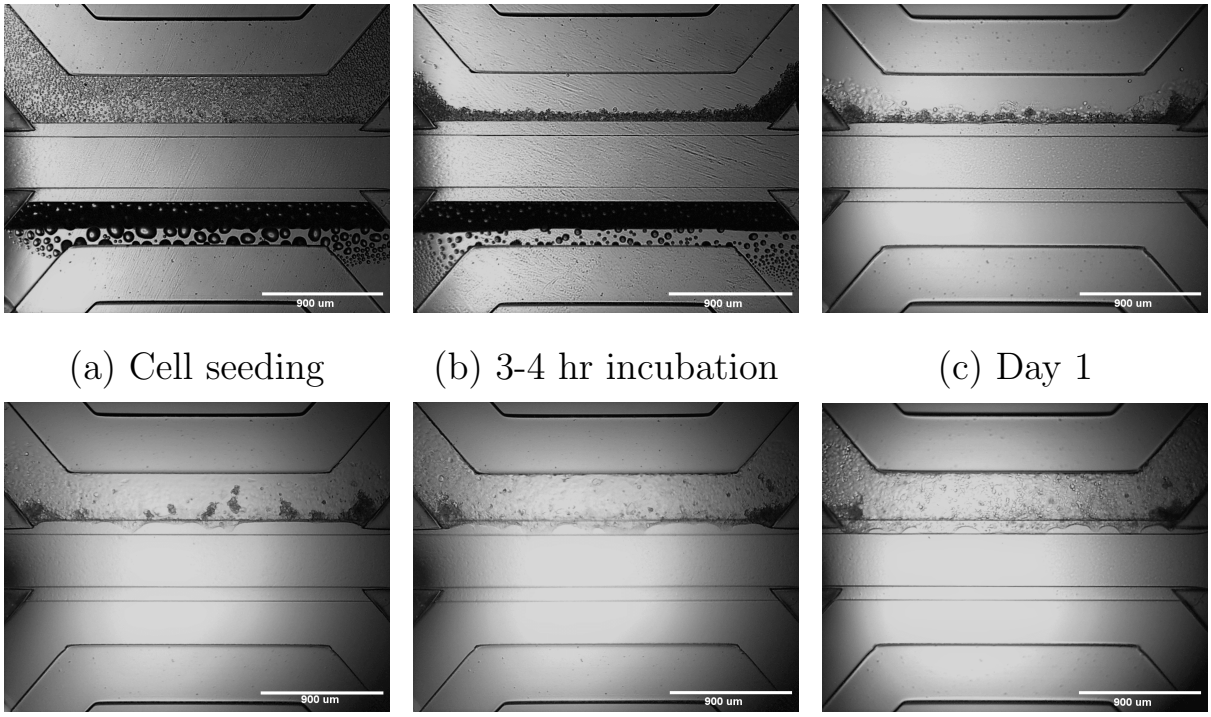

(a) Cell seeding (b) 3-4 hr incubation (c) Day 1

(d) Day 2 (e) Day 3 (f) Day 4

Figure 10: **Cell seeding of chips in the organoplate**. **a.** Cell lane perfused with cell suspension. **b.** Chip after 3-4 hour incubation horizontally. **c-f.** Cells growing in the chip from 1 to 4 days after seeding, resulting in fully grown and differentiated cell tubule.

figure 10a. As seen in the figure the cell channel is completely full. To enable the cells to attach to the ECM, the plate is placed in a holder horizontally for 3-4 hours. In figure 10b the chip after 3-4 hours placed horizontally can be seen. The cells are all located toward the ECM. Over the next four days, the cells start to proliferate and differentiate which can be seen in figure 10c-10f. After 4 days the cells are fully grown and differentiated and are ready to be used.

3.2.2 Cell characterization

To confirm that the cells have successfully differentiated and polarized, immunofluorescence staining is carried out. Fully differentiated and polarized cells exhibit tight junctions between and adjacent cells, while on the apical brush border formation of microvilli takes place. To be able to visualize and confirm the presence of these characteristics, immunostaining with ZO-1 and ezrin has been done. ZO-1 is a marker of tight junction formation, while ezrin is a marker of the brush border formation.[57] In figure 11a and 11b

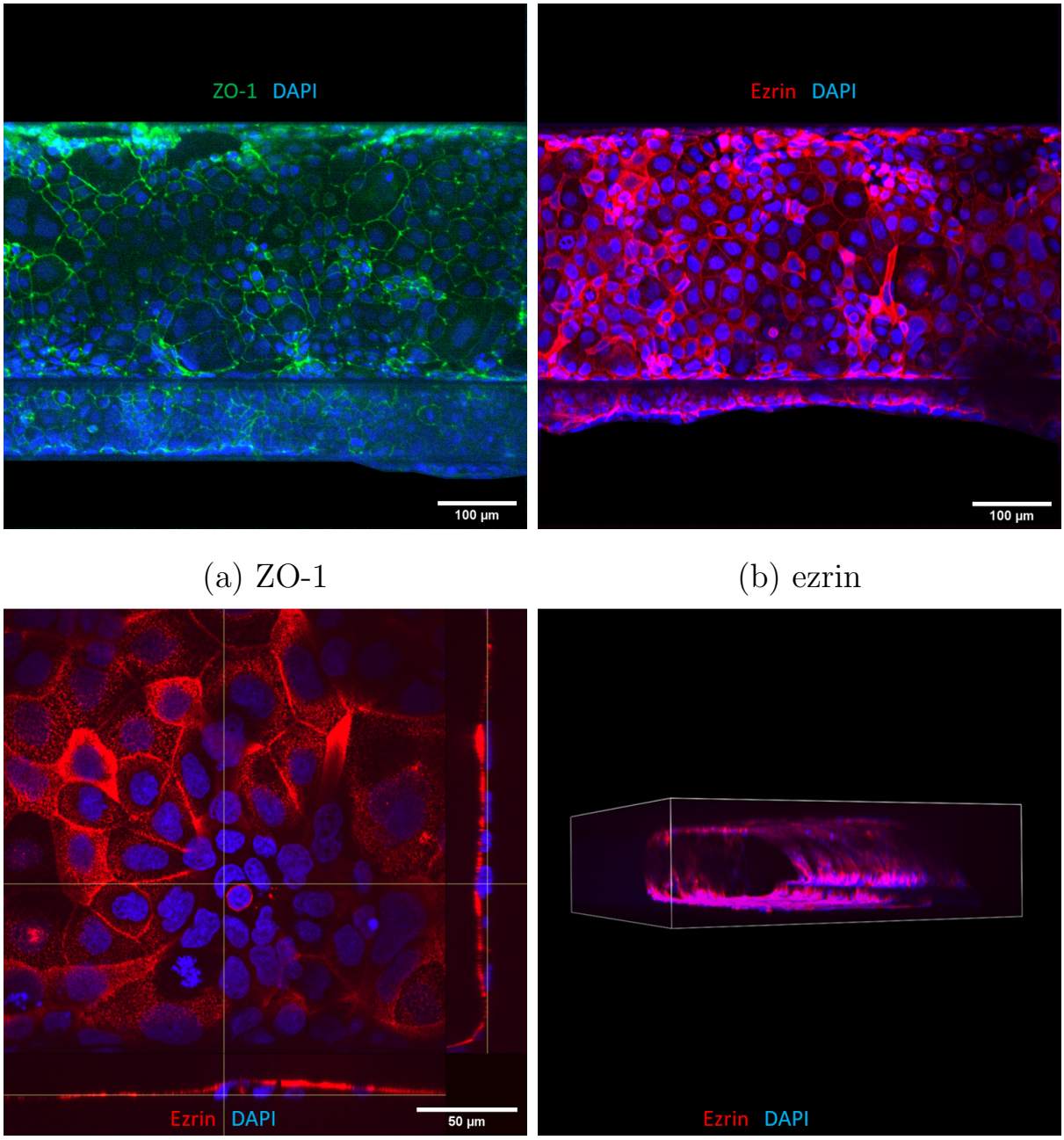

(a) ZO-1

(b) ezrin

(c) Ezrin cross section

(d) ezrin tube

Figure 11: **Immunostaining confirming tight junction and brush border formation in Caco-2 tubules**. Immunostaning carried out along with staining of the nuclei with dapi. **a.** Maximum intensity projection of ZO-1 stain showing the formation of tight junctions. **b.** Maximum intensity projection of ezrin stain showing the formation of the brush border. **c.** Zoomed cross section showing the polarization of the cells. **d.** Z-stack 3D image of the cell lane showing the formation of a tubular structure.

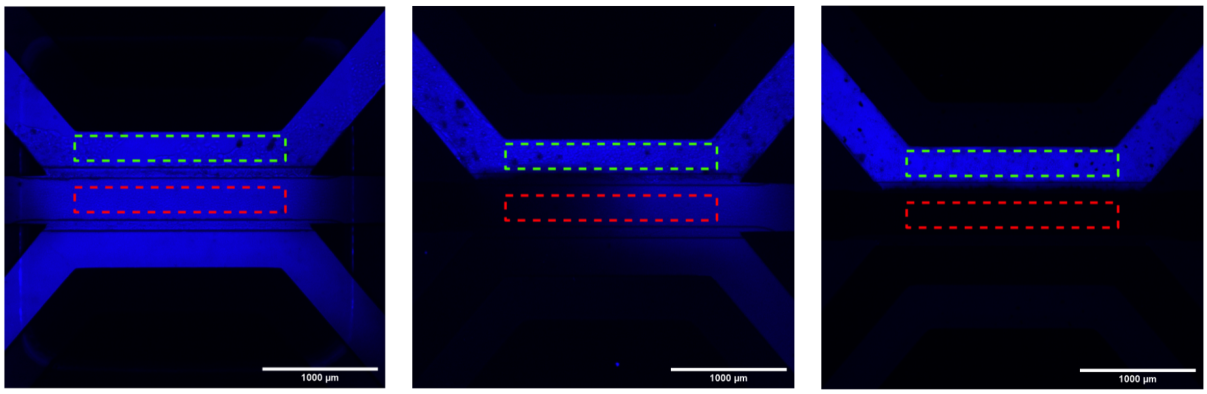

(a) Leaky (b) Part leaky (c) Tight

Figure 12: **Barrier integrity imaging of leaky, part leaky and tight Caco-2 tubules**. Barrier integrity imaging using TD and SDCM. **a.** Leaky cell barrier where the TD have leaked through and covers the whole chip. **b.** Partly leaky barrier, in which the TD have only partly leaked through. **c.** Tight cell barrier, in which the TD is retained in the lumen of the tube.

the maximum intensity projection can be seen for ZO-1 and ezrin, respectively. ZO-1 is located in between the cells indicating the formation of tight junctions between adjacent cells. Compared to the ezrin stain, more smeared-out staining is present, as the ezrin is only located on the apical brush border side of the cell layer. This can be seen more clearly in figure 11c where a zoom in and more closely looks at the location of the ezrin stain can be seen. A cross-section view at the indicated lines can be seen on the right side and bottom of the figure. Here it is clearly seen how the ezrin is forming a layer on top of the nuclei, thereby covering the nuclei. No ezrin is seen beneath the cells, which is an indication of cells have successfully differentiated and polarized during the 4 days of growth in the chip. In figure 11d is a 3D side-view through the entire cell lane showing the formation of the Caco2 tubule. Both the staining of the nuclei and the brush border are seen forming a tubular structure, with the inside being the lumen.

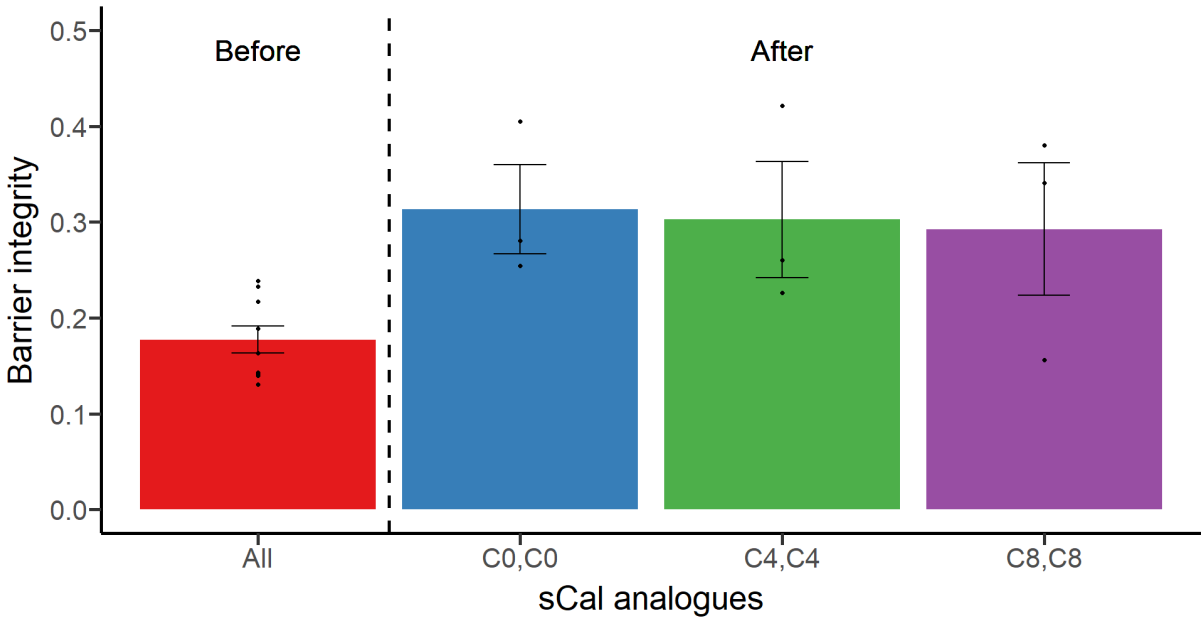

Figure 13: **Barrier integrity measurements before and after translocation experiment showing increasing BI after experiment**. The barrier integrity measurements using TD and SDCM. Errorbars calculated as standard error of the mean with n=9 before and n=3 after.

3.3 Translocation study using SDCM display internalization and accumulation of sCal(C8,C8).

3.3.1 Barrier integrity measurements

To confirm the formation of intact Caco-2 tubules the barrier integrity of the tubules is examined. The barrier function of the Caco-2 tubules grown over 4 days is examined by perfusion of TRITC-dextran (4.4kD) (TD), a fluorescent glucose molecule in culture medium, through the tube lumen. In figure 12 Three different scenarios can be seen. In figure 12a a leaky cell barrier is shown. The TD has leaked into the ECM lane and the whole chip fluoresce. In figure 12b the cell barrier is only partly leaky, which causes part of the ECM lane to fluoresce. In figure 12c a complete tight cell barrier is seen. The TD is retained in the lumen of the tube, which causes only this lane to fluoresce. The fluorescence signal in the ECM lane (red dotted square in figure 12) normalized to the fluorescence signal in the lumen (green dotted square in figure 12) is then determined as the BI. For a leaky cell barrier, the signal in the ECM and lumen will be almost equal giving a BI≈1. For cell tubules with BI>0.4 the barrier integrity of tubules is considered

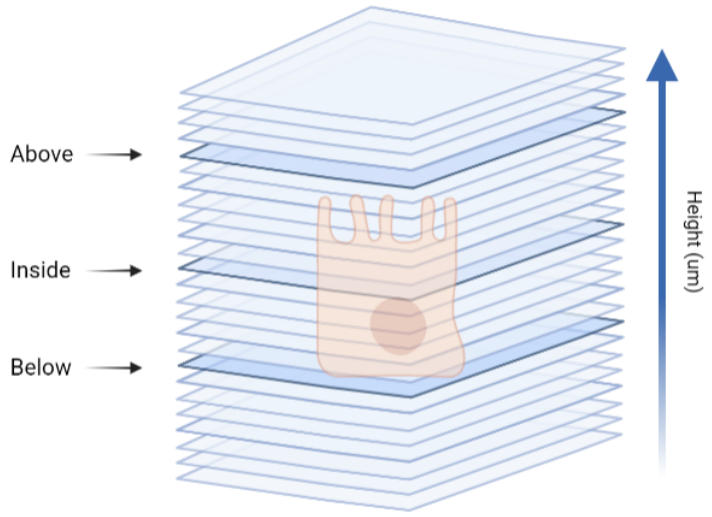

Figure 14: **Schematic illustration of z-stack measurements performed on the SDCM and extraction of slices.** Using the SDCM, z-stacks of 0.5μm thick steps was imaged from below the cells to above the cells. Three slices corresponding to at the bottom, inside and above the cell are extracted for further analysis.

lost [57] and are discarded.

The BI of Caco-2 tubules used for the translocation experiment can be seen in figure 13. The BI of Caco-2 tubules are measured both before and after the experiment. Each data point is plotted with black points. Prior to the experiment the BI of the tubules are all below 0.3 with a mean of 0.18 and are therefore considered to have a tight cell barrier. After the performed experiment the BI of Caco-2 increases, which is consistent for all peptide analogs. The mean of the BIs is still below the limit of being considered tight of 0.4, for each peptide analog. Though looking at the individual data points reveals that a single Caco-2 tubule actually reaches the limit and slightly exceeds the limit of 0.4.

3.3.2 SDCM data extraction and analysis

To track the translocation of sCal analogs over time, the location of the peptide analog over time is determined. To detect the peptide localization below the cell layer, inside the cells and above the cells, in the solution, z-stack imaging using SDCM is performed which is illustrated in figure 14. To follow the location over time, z-stack imaging is done every 40 min for 4 hours. Only intact cell tubules are used to investigate the translocation of the peptide analogs over time. The study is carried out using sCal(C0,C0), sCal(C4,C4)

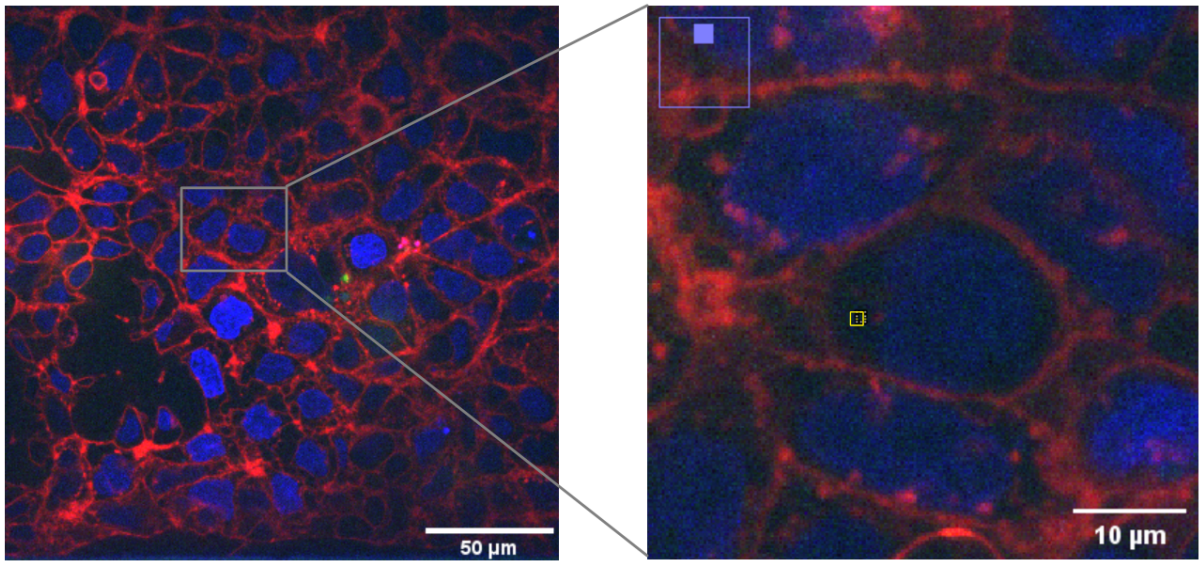

Figure 15: **Analysis of z-stack obtained from SDCM and illustration of creation of ROIs.** Z-stacks are recorded using SDCM. ROIs (yellow square) are made in the cytosol using FIJI. Intensities of the nuclei, membrane and the peptide analog in the ROIs are extracted as mean pixel intensities and used for further analysis.

and sCal(C8,C8) with concentrations of 1μM, 1μM and 0.5μM, respectively. The lower concentration of sCal(C8,C8) is due to low stock concentration. Z-stacks of 0.5μm thick steps from below the cells and up in the solution above the cells, monitoring signals of the nuclei, membrane, and peptide analog, are recorded. Figure 15 is an example of a single slice of a z-stack. The nuclei are seen in blue, while the membrane is seen in red. To analyze the translocation of peptide analogs, small regions of interest (ROIs) in the cytosol of the cells are made as can be seen at the zoom in to the right in figure 15. Every ROI is carefully checked that it was placed in the cytosol of cells at every time point. Since it is live-cell imaging, the cells could move around during the 4 hours, which caused great need of attention during this process. The signal of the nuclei, membrane, and peptide analog was extracted for the entire z-stacks monitored over time.

Implementation of scripts, seen in section 7.8, allows analysis of extracted data. Starting by looking at the membrane signal, it is possible to determine the position of the cells. Viewing the membrane signal as a function of the height of the z-stack will produce a plot with two peaks, one at the bottom of the cells and one at the top of the cells as seen in figure 16a. The experiment is carried out for 4 hours, with imaging every 40 min, which is represented in the color scale of the plot. As can be seen in figure 16a, the peaks

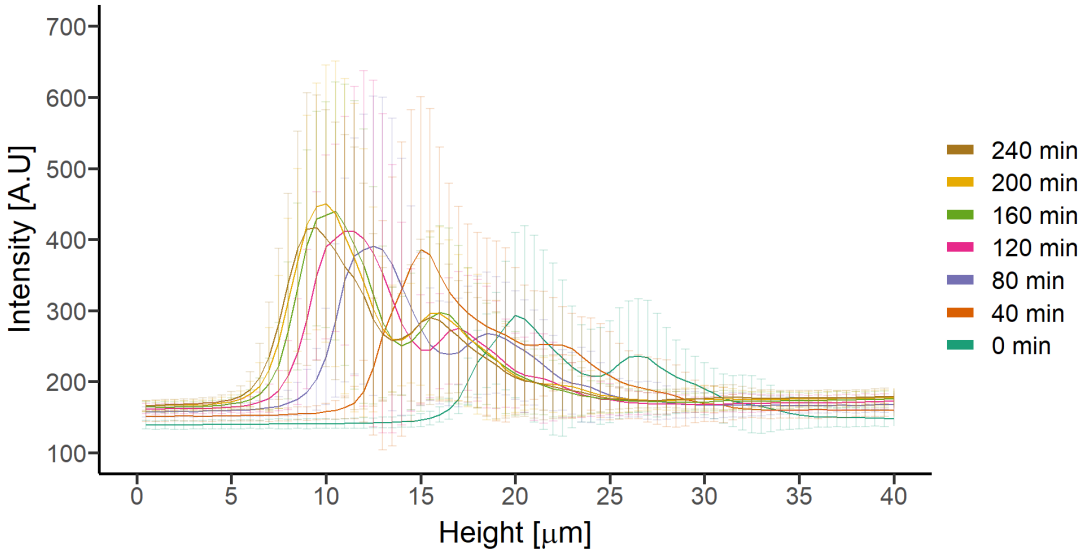

(a) Membrane signal

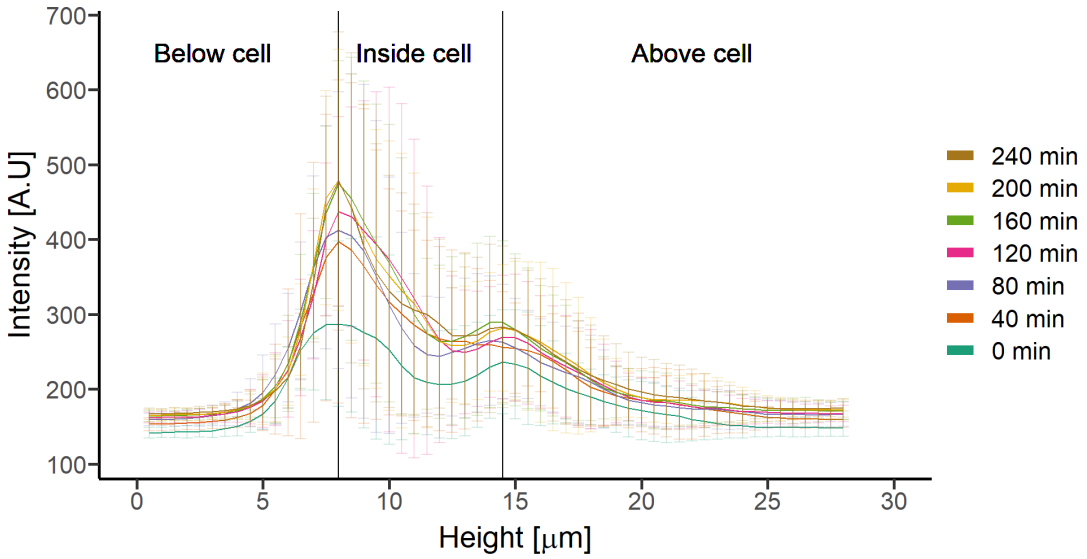

(b) Alignment of membrane signal

Figure 16: **Alignment of membrane signal as function of height to determine position of the cells.** Membrane signal tract over 4 hours using SDCM **a.** Original membrane signal as function of height, showing need of alignment to determine cell position. **b.** Alignment of membrane signal and determination of cell position. Black line indicate cell position.

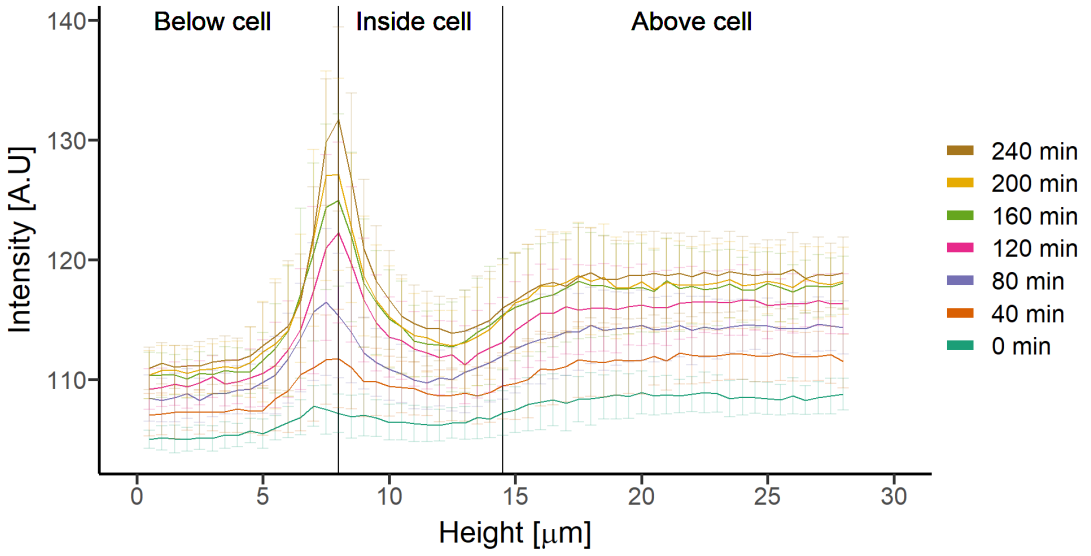

Figure 17: **Extraction and alignment of peptide signal as function of height.** Peptide signal tract over 4 hours using SDCM. Alignment of peptide signal based on cell position was done. Cell position indicated by black lines..

are moving over time which is due to the temperature of 37°C. This presents the need for alignment of the signal, to ensure the correct determination of the position of the cells. The result of the alignment can be seen in figure 16b, with the black lines indicating the bottom and the top of the cells, respectively. Figure 16 shows a single example of one of the experiments performed. This alignment has been implemented for all the experiments carried out. Following the determination of the cell position based on the membrane signal, the peptide signal was encountered. Applying the same alignment as for the membrane signal, ensuring the same position of the cells. In figure 17 the aligned peptide signal can be seen as the function of the z-stack height. As with the membrane signal, the vertical black lines indicate the bottom and the top of the cells. Again the color scale corresponds to the time point of measurement during the 4-hour experiment. For this particular example, a peak is at the bottom of the cells, though it is difficult to contemplate the translocation over time.

3.3.3 Relative translocation analysis

To better visualize the translocation of the peptide analogs over time three areas of interest are picked out from figure 17. The areas of interest are to establish the translocation at 1. the bottom of the cells, 2. At the inside of the cells and 3. above of the cells.

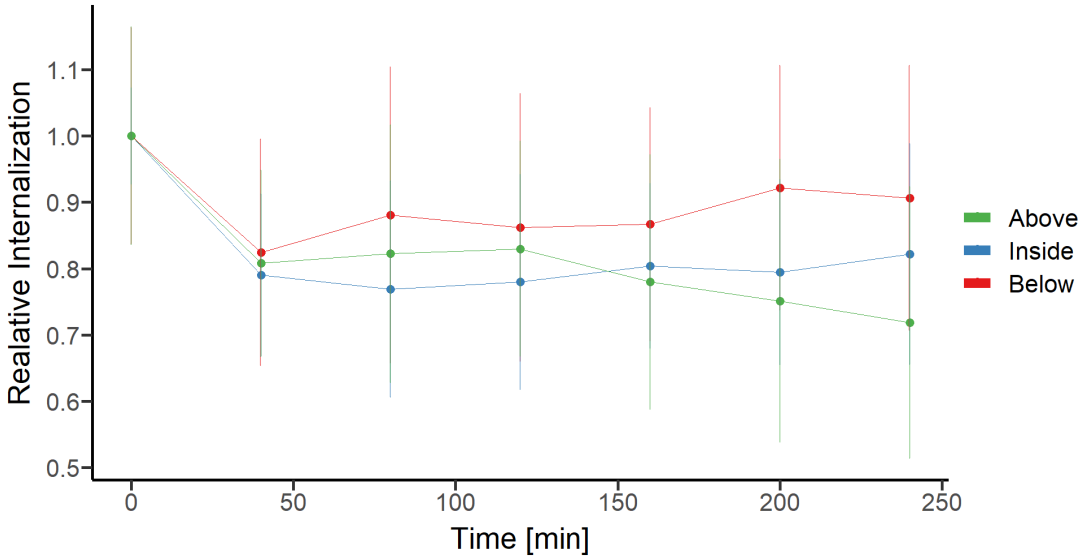

Figure 18: **Peptide signal of sCal(C0C0) over time showing no indication of translocation.** Extraction peptide signal of sCal(C0,C0) at the bottom, inside and above the cells tract for 4 hours using SDCM. Normalized to first data point showing relative translocation. Errorbars calculated as standard error of the mean with n= 3.

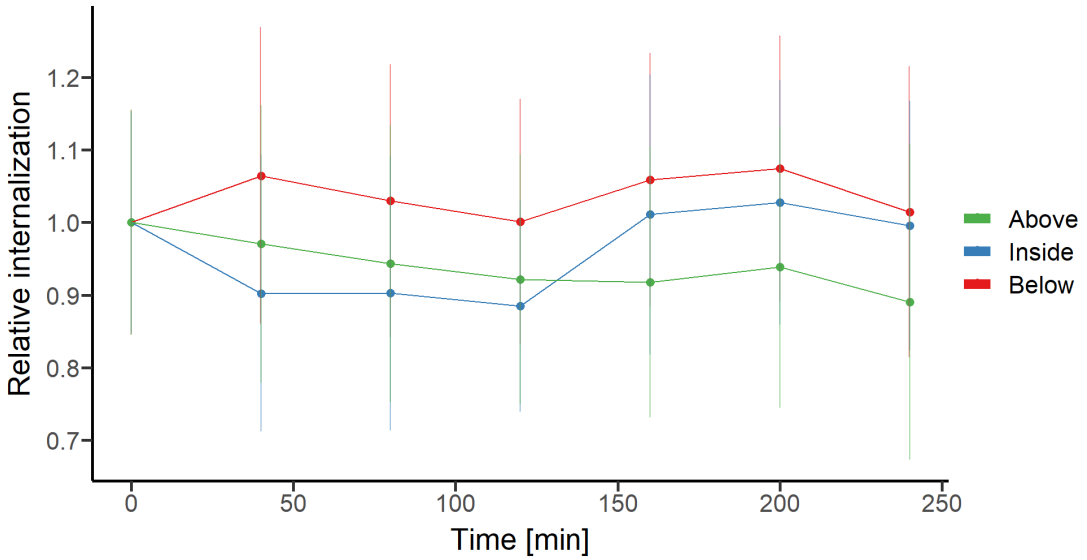

Figure 19: **Peptide signal of sCal(C4C4) over time showing no indication of translocation.** Extraction peptide signal of sCal(C4,C4) at the bottom, inside and above the cells tract for 4 hours using SDCM. Normalized to first data point showing relative translocation. Errorbars calculated as standard error of the mean with n= 3.

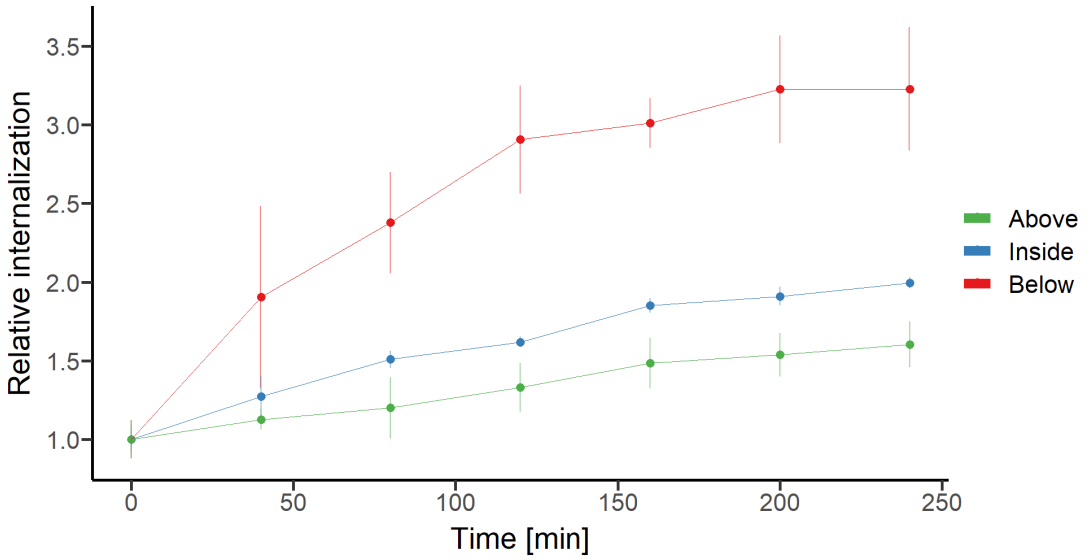

Figure 20: **Peptide signal of sCal(C8C8) over time showing indication of translocation and accumulation at the bottom of the cells.** Extraction peptide signal of sCal(C8,C8) at the bottom, inside and above the cells tract for 4 hours using SDCM. Normalized to first data point showing relative translocation. Errorbars calculated as standard error of the mean with n= 3.

Slices from the z-stacks corresponding to these three areas are extracted as illustrated in figure 14. In figure 18, 19 and 20 the relative translocation over time can be seen for sCal(C0,C0), sCal(C4,C4) and sCal(C8,C8), respectively. The peptide signals are shown as a function of time, with the color scale corresponding to each of the three locations relative to the cells. The peptide signal has been normalized to the first measurement (first time point) at each of the three locations. In this way, the progression of the signal relative to time = 0 can be seen.

In figure 18 the peptide signal of sCal(C0,C0) at the three locations is seen. A drop in intensity after the first 40 minutes is seen at all three locations to around 80% of time = 0. Though considering the errorbars, no significant difference is relative to time = 0. Considering the signal of sCal(C4,C4), which is seen in figure 19 the same tendency as for sCal(C0,C0) is seen. Due to the large errorbars, the fluctuations over time are considered insignificant and essentially the signal at all three locations are constant over time. Turning the attention to the signal of sCal(C8,C8), seen in figure 20, something interesting is happening. The signal both inside and below the cells are increasing over time. The steepest increase is seen below the cells and increases to almost 3.5 times the

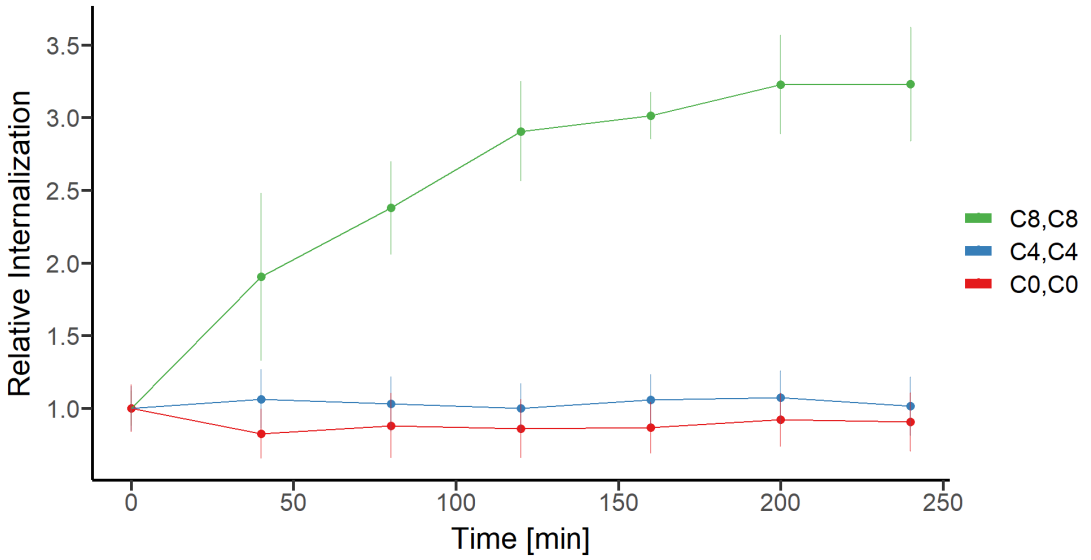

Figure 21: **Peptide signal as function of time at the bottom of the cells indicate translocation of sCal(C8,C8).** Extraction of peptide signal at the bottom of the cells for each peptide analog, tract over 4 hours using SDCM. Normalized to first data point showing relative translocation. Errorbars calculated as standard error of the mean with n= 3.

signal at time = 0. The errorbars are smaller and not overlapping, as for sCal(C0,C0) and sCal(C4,C4), which indicates a significant difference between the three locations.
To better compare the three peptide analogs, the signal below the cells has been extracted for each of them and collected in figure 21. Like the three previous figures, the normalized intensity is plotted as a function of time. Here the color scale now represents the three peptides with sCal(C0,C0), sCal(C4,C4) and sCal(C8,C8) in red, blue and green, respectively. The similarity between sCal(C0,C0) and sCal(C4,C4) is even more clearly seen. For both peptide analogs the signal is constant over time. Hence no indications of the peptide analogs being internalized by the cells are seen. As the similarity of sCal(C0,C0) and sCal(C4,C4) is more clearly seen, the difference of the signal of sCal(C8,C8) is also seen. Compared to sCal(C0,C0) and sCal(C4,C4), sCal(C8,C8) an increase of signal is seen through the entire time period. The signal below the cells for each peptide at time = 240 min has been extracted and can be seen in figure 22. The individual data points are included along with the standard error of the mean. Student t-tests are performed between sCal(C0,C0) with sCal(C4,C4) and sCal(C0,C0) with sCal(C8,C8) obtaining p-values of 0.253 and 0.021, respectively. This means at a 5% significance level, there is no

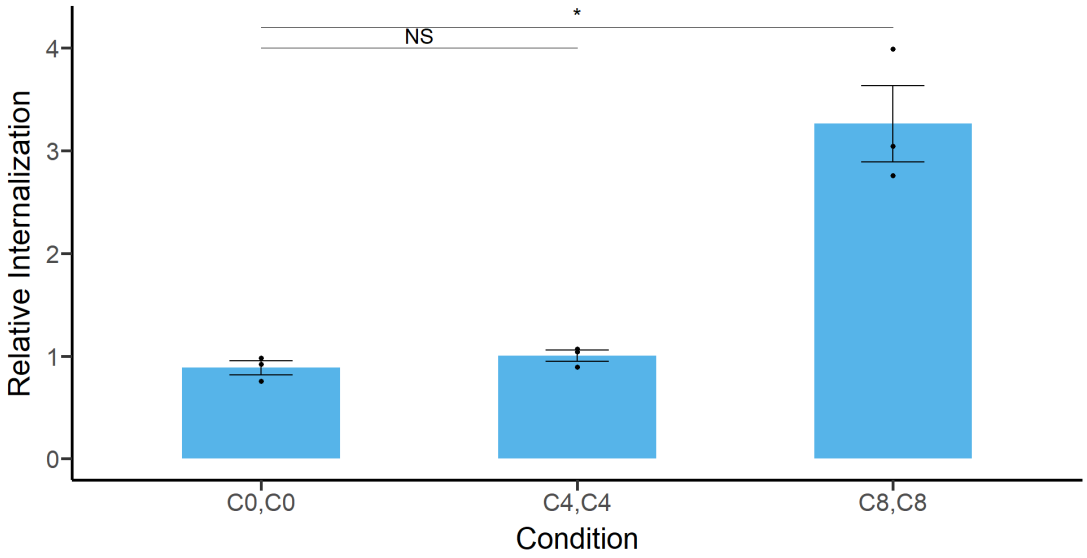

Figure 22: **Peptide signal at the bottom of the cells show significant difference between sCal(C0,C0) and sCal(C8,C8) after 240 min.** Extraction of endpoint peptide signal tract using SDCM for 4 hours. Normalized to first data point showing relative translocation. Student t-test performed on sCal(C0,C0) with sCal(C4,C4) and sCal(C0,C0) with sCal(C8,C8) revealing p-values of 0.830 and 0.018, respectively.

significant difference between sCal(C0,C0) and sCal(C4,C4). On the contrary the p-value confirms a significant difference between sCal(C0,C0) and sCal(C8,C8).

3.4 Transport study using WFM display significant concentrations dependency of sCal(C0,C0) and sCal(C4,C4).

Following the investigation of the translocation of the three peptide analogs, the transport across the cell tubule of the same peptide analogs is examined. Using WFM imaging of the whole chip detection of how much peptide made it out of the cell lane, through the cell barrier, and into the ECM lane is monitored as illustrated in figure 23. On the left side is the cell tubule which gets perused with a peptide solution illustrated by the green shade. The transport of the peptide analogs is recorded using WFM and the mean pixel intensity of an area in the ECM lane, illustrated by red dotted square, is extracted. Both the signal of the peptide analogs and the TD is extracted. In this way, the transport of both the peptide analogs and TD can be analyzed. As previously, the barrier integrity of the cell tubules is measured, ensuring only cell tubules with an intact cell barrier and a barrier integrity below the limit of 0.4 are used.

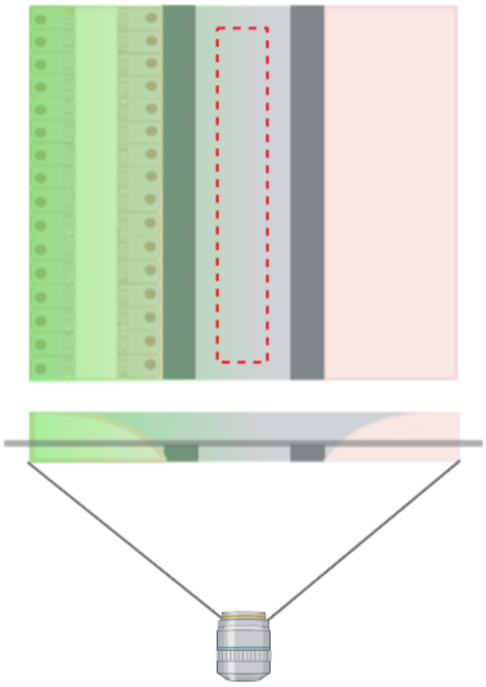

Figure 23: **Illustration of widefield setup and performed intensity measurements.** Schematic illustration of the view obtained through the widefield microscope. To the left is the cell lane and the ECM lane is in the middle. Phaseguides are illustrated in dark grey, while the solution of peptide analogs is represented by the shaded green color. The mean pixel intensity signal have been measured in the area of the red dotted field of both the peptide analogs and TD.

Hence the possibility of the peptide analogs transported across the cell barrier due to the cell barrier being leaky or partly leaky is diminished. Along with monitoring the signal of the peptide analogs, the signal of TD is also monitored. By including TD, the integrity of the cell barrier is monitored simultaneously to the transport of the peptide analogs. In this way, it is possible to determine the effect of the peptide analogs on the integrity of the cell barrier. Since TD is included and the intensity of this is detected throughout the experiment, the barrier integrity was not measured after the experiment.

3.4.1 Relative transport at low concentration

The transport experiments are first carried out with the same concentrations as used for the translocation experiments, meaning 1μM, 1μM and 0.5μM for sCal(C0,C0), sCal(C4,C4) and sCal(C8,C8), respectively, along with a control consisting of the trans-

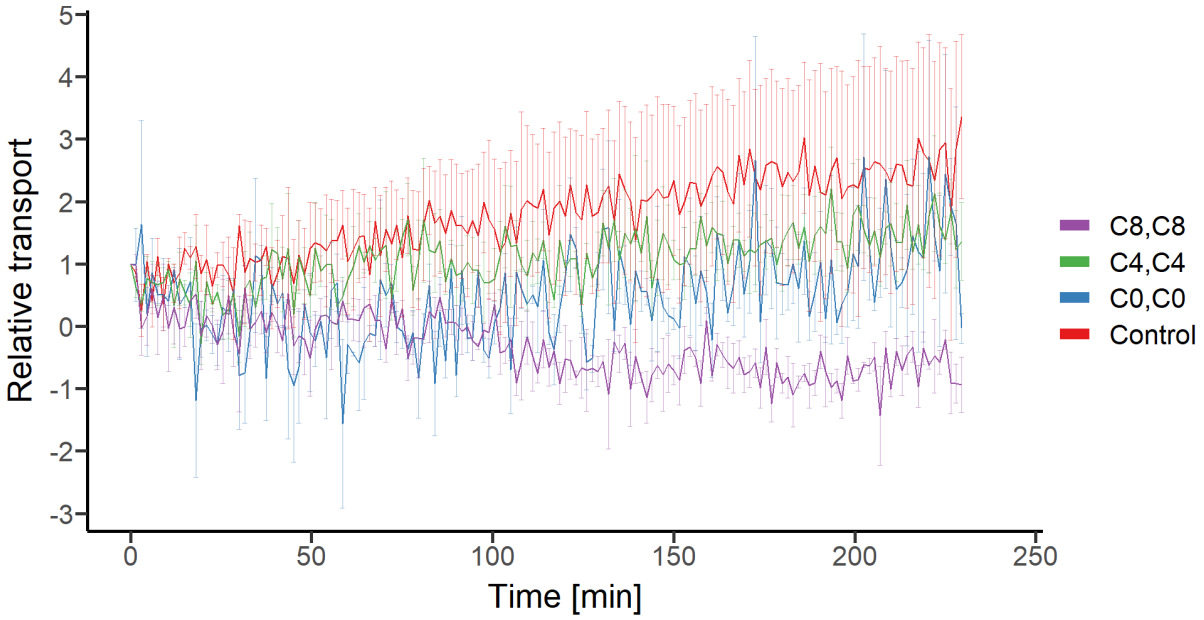

(a) Peptide signal

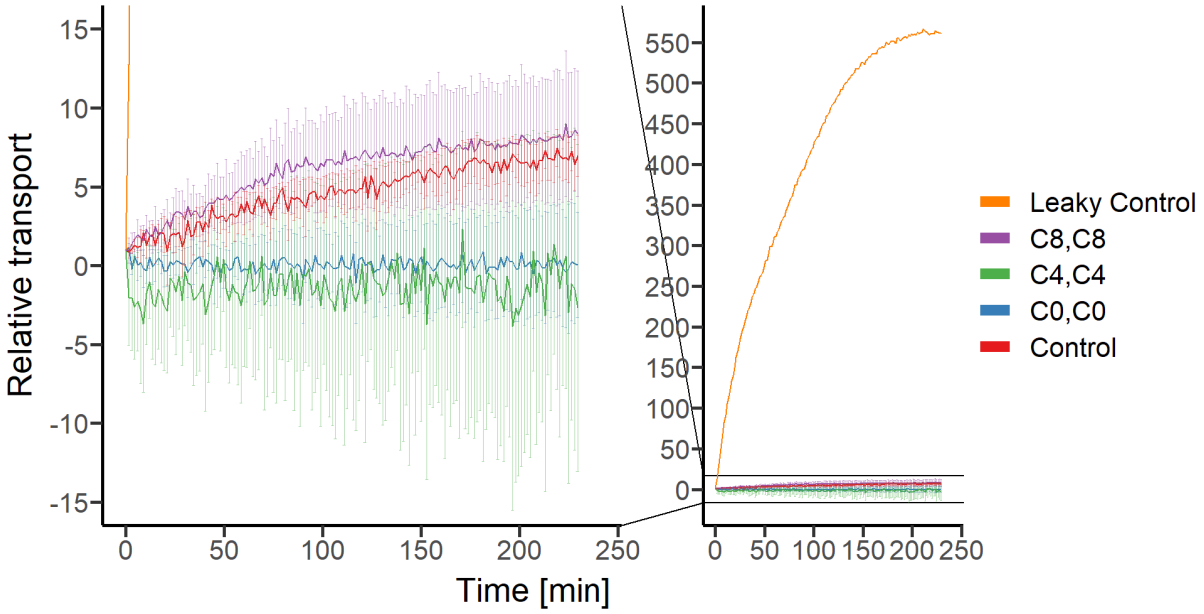

(b) TRITC-dextran signal

Figure 24: **Relative transport of the peptide analogs at low concentration indicates intact cell tubules, though no transport after approx. 4 hours.** Peptide and TD signal tract over hours using wide-field microscopy. Normalized to first data point showing relative transport over time of **a.** peptide signal and **b.** TD signal. Errorbars calculated as standard error of the mean with n= 3.

port media with TD. The lower concentration of sCal(C8,C8) is due to low stock concentration. The intensities of both the peptide signal and the TD signal over time are extracted and analyzed using scripts seen in section 7.8. In figure 24a the peptide signal as a function of time for the three peptide analogs and the control is showed. The color scale corresponds to each peptide analog and the control. The signals are normalized to the first time measurement, to see the evolvement through time. A similar tendency for sCal(C0,C0) and sCal(C4,C4) peptides is seen. In the first 100 min of the experiment, the relative signal is rather constant, while after 100 min a small increase is seen for the rest of the experiment. The relative signal increases to around 2. It is though important to compare to the control, which does not contain peptides. The control is seen to have a steady increase throughout the entire experiment. Comparing the control with sCal(C0,C0) and sCal(C4,C4), the control is seen to have a higher relative transport throughout the entire experiment. Looking at sCal(C8,C8) the signal is seen to have a steady decrease over time. Though the decrease is in the same range as the increase seen for sCal(C0,C0) and sCal(C4,C4). Overall the relative signal of all three peptide analogs is less than the relative signal of the control. Due to the large uncertainties displayed by the errorbars, the signal of all peptide analogs and the control is considered constant through time.

The relative TD signal as a function of time for the three peptide analogs is seen in figure 24b. Again the color scale corresponds to each peptide analog and the controls. Two control, consisting of transport medium with TD, are included. The first control denoted "control" is added to a tight cell tubule, while the second control, denoted "leaky control" is added to a leaky cell tubule. The TD transport in the leaky control is seen to reach a fold increase above 550. Comparing the TD transport of the peptide analogs and the control shows a significant difference. To the left of figure 24b is a zoom-in on the TD transport for the peptide analogs and the control. For sCal(C0,C0) and sCal(C4,C4) the relative TD signals are constant through the experiment, though large errorbars is especially seen for sCal(C4,C4). These errorbars are in the negative range, which indicates that the cell tubule stays intact after the addition of sCal(C4,C4), which is also the case for sCal(C0,C0). Comparing with the control an increase of the relative signal up to 5 is seen. the TD signal of sCal(C8,C8) is placed slightly higher than the control. Though due to large errorbars no significant difference is seen between the control and

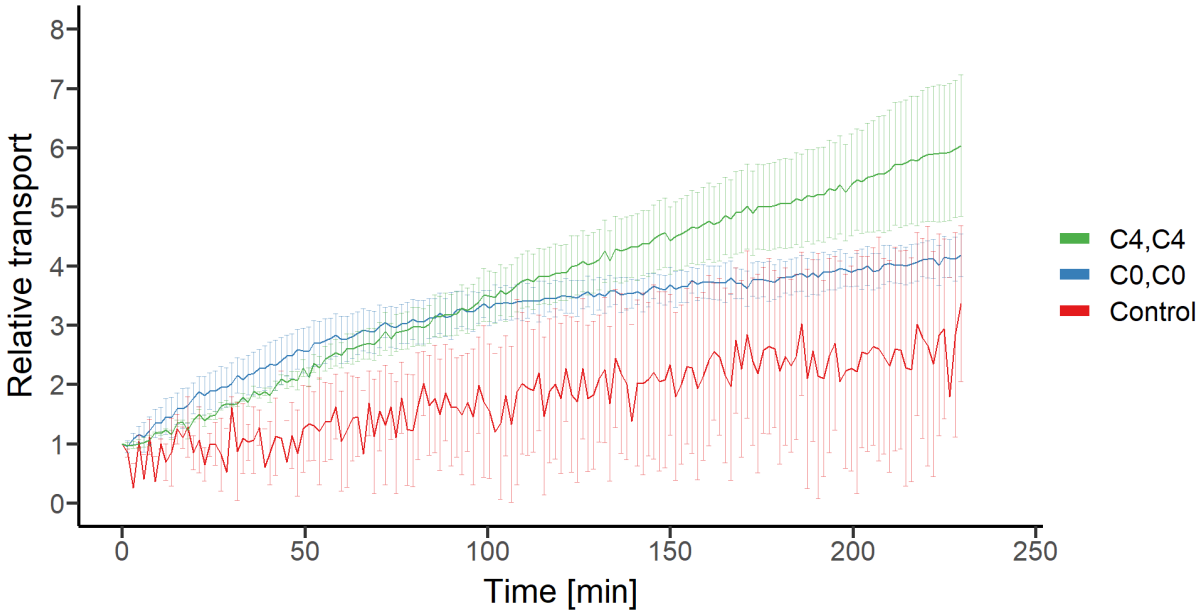

(a) Peptide signal

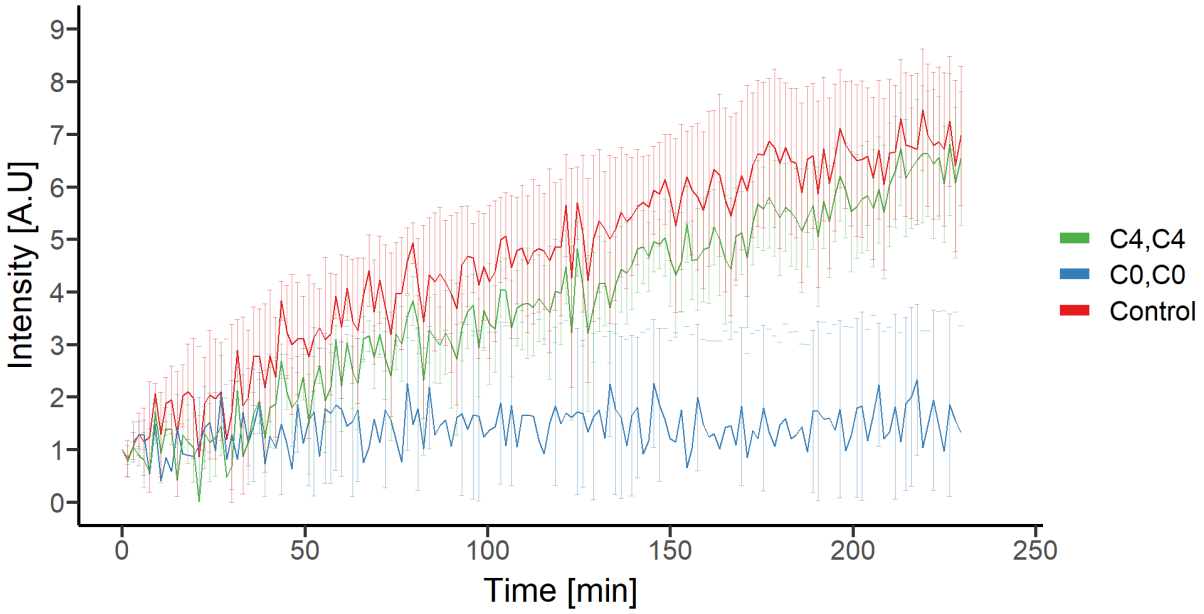

(b) TRITC-dextran signal

Figure 25: **Relative transport of the peptide analogs at high concentrations indicates intact cell tubules and transport after approx. 4 hours.** Peptide and TD signal tract over hours using wide-field microscopy. Normalized to first data point showing relative transport over time of **a.** peptide signal and **b.** TD signal. Errorbars calculated as standard error of the mean with n= 3.

sCal(C8,C8).

3.4.2 Relative transport at high concentration

After not seeing any transport of either of the peptide analogs with the low concentration it would be interesting to investigate if the transport of the peptide analogs is dependent on the concentration. To investigate this, the concentration of the peptide analogs is increased to 10μM. The experiments are only carried out with sCal(C0,C0) and sCal(C4,C4) due to low stock concentration of sCal(C8,C8). In figure 25a the relative peptide signal as a function of time for the two peptide analogs along with the control is seen. As previously the color scale corresponds to which peptide analogs and the control. Starting by looking at sCal(C0,C0) a steep increase in the first 50 min is seen, while after the 50 min the increase flattens out. Comparing with sCal(C4,C4), another tendency is seen. Here a close to linear increase is seen through the entire experiment and the end intensity reaches a higher level. In relationship to the control, there is a clear difference.

In figure 25b the relative signal of TD seen for the experiment carried out with the concentration of 10μM. Again the color scale corresponds to the control and peptide analogs. Only the control of the tight cell tubule is included. The relative TD signal of both peptide analogs is seen to be less than what is seen for the control. Though while the relative signal for sCal(C0,C0) is almost constant over time, the relative signal of sCal(C4,C4) increases with a similar slope as the control. The relative signal of sCal(C4,C4) never exceeds that of the control.

3.4.3 Concentration dependency of relative transport

To better investigate the concentration dependency of the transport of the peptide analogs, the relative peptide signal of the peptide analogs at the two different concentrations, along with the control, over time is seen in figure 26a. Notice that compared to earlier the color scale has now changed since the same peptide is included at two different concentrations. Based on this figure a clear concentration dependency is seen. While the control and the peptide analogs at 1μM have relative peptide signals of less than 2, the sCal(C0,C0) and sCal(C4,C4) at 10μM have relative peptide signals of around 4 and 6, respectively. In figure 26b the comparison of TD between concentrations is seen. The same color scale is

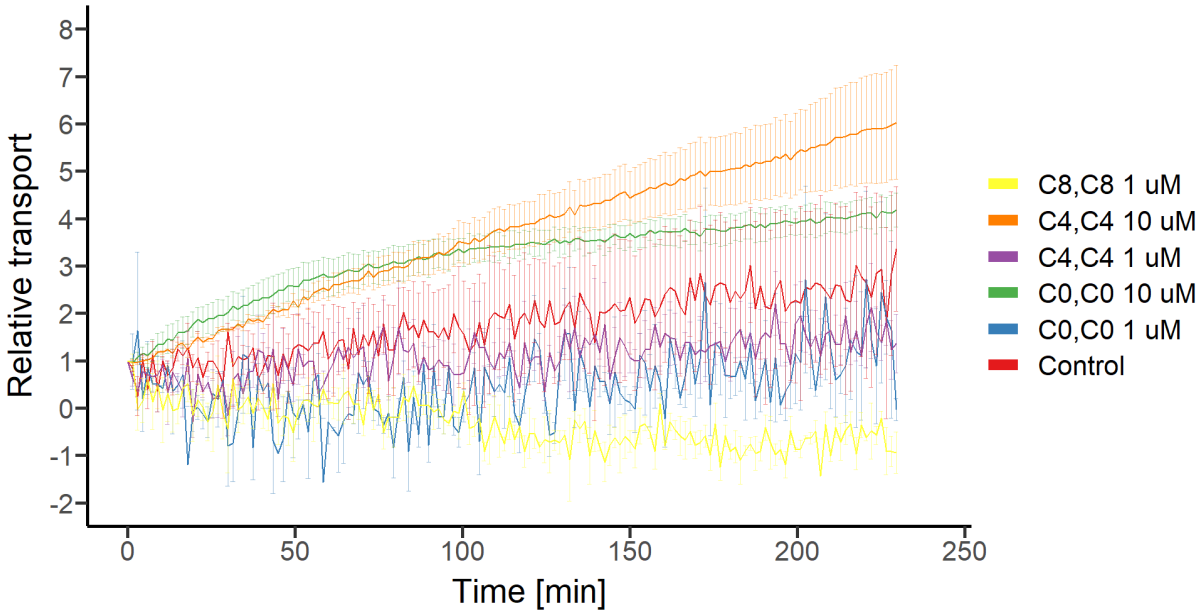

(a) Peptide signal

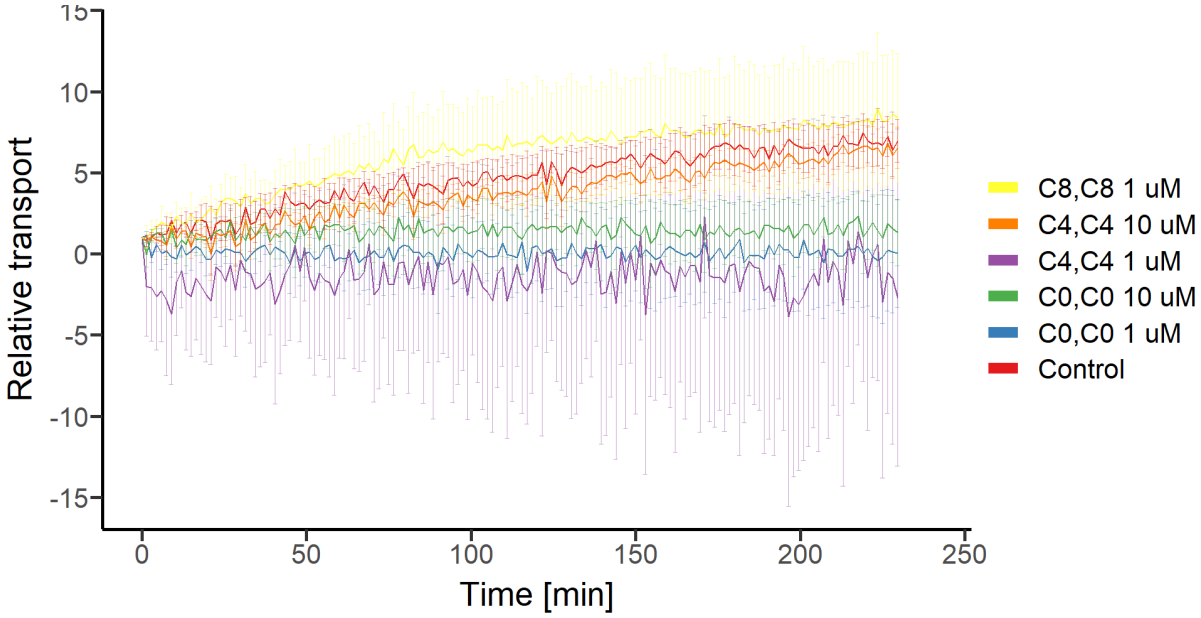

(b) TRITC-dextran signal

Figure 26: **Relative transport of the peptide analogs at both concentrations indicates intact cell tubules and concentration dependent transport after approx. 4 hours.** Peptide and TD signal tract over hours using wide-field microscopy. Normalized to first data point showing relative transport over time of **a.** peptide signal and **b.** TD signal. Errorbars calculated as standard error of the mean with n= 3.

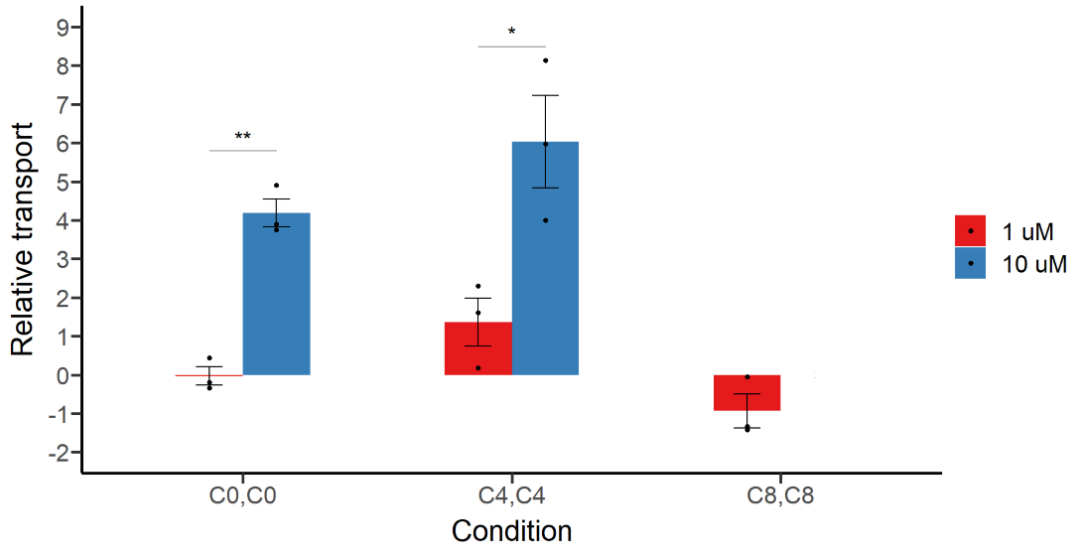

Figure 27: **Relative peptide signal after approx. 4 hours shows significant concentration dependency of sCal(C0,C0) and sCal(C4,C4).** Extraction of endpoint peptide signal tract using wide-field microscopy for hours. Normalized to first data point showing relative transport. Errorbars calculated as standard error of the mean with n= 3. Student t-test examination of concentration dependency of sCal(C0,C0) and sCal(C4,C4) revealing p-values of 0.0012 and 0.0403, respectively.

used as for figure 26a. Again only the control of the tight cell tubule is included. As also seen earlier at low concentrations of 1μM and even up to a concentration of 10μM the TD signals of the peptide analogs are lower than the control, except sCal(C8,C8) which is much similar to the control without any significant difference.

To investigate the significance of the concentration dependency, the relative peptide signal at the end time of the experiments are extracted and seen for each peptide analogs in figure 27. Relative transport corresponding to a concentration of 1μM is seen in red, while relative transport corresponding to a concentration of 10μM is seen in blue. The plot is divided according to the peptide analogs. Due to relatively large errorbars, the individual data points are added (black dots). Student's t-tests between peptide analogs at each concentration are done. This showed at a 5% significance level a significant difference between sCal(C0,C0) and sCal(C4,C4) at each concentration with p-values of 0.0012 and 0.0403. The p-value of 0.0403 of sCal(C4,C4) at each concentration, is on the border of significance, which is due to the large errorbars at both concentrations. The large errorbars are caused by the widespread of each data point for each experiment. This is

not seen to the same extent for sCal(C0,C0) where each data point is closer to each other. Student t-test has also been performed to see if there are significant differences between peptide analogs within the same concentrations. Though at a significance level of 5%, no significant differences are observed.

4 Discussion

Previous work done by Trier et al.[12] showed that single lipidation could induce transport of sCal. In this study, the concept is expanded to investigate double lipidation of sCal. Furthermore, this study takes advantage of the emerging organ-on-a-chip system, allowing live-cell imaging of internalization, translocation and transport of sCal analogs.

4.1 Concentration and lipid length dependency on cytotoxicity

A Pierce LDH cytotoxicity assay is performed on five sCal analogs, with increasing lipid lengths, at five different concentrations going from 5μM to 75μM. As seen in figure 9 sCal(C0,C0) and sCal(C4,C4) showed no significant differences to the control, which did not contain peptide, at any of the concentrations. In this range no concentration dependency on the cytotoxicity. is observed for sCal(C0,C0) and sCal(C4,C4). The lipidation of lipid lengths C4,C4 did neither influence the cytotoxicity. Increasing the lipid length to sCal(C8,C8), sCal(C12,C12) and sCal(C16,C16) a significant concentration dependency on the cytotoxicity is observed, in one case reaching a cytotoxicity around 80%. At lower concentrations (5μM and 10μM) sCal(C12,C12) also shows significant higher cytotoxicity compared to sCal(C8,C8) and sCal(C16,C16). The cytotoxicity of lipidated sCal is both dependent on lipid length and concentration at lipid lengths greater than C8,C8.

4.2 Lipid length dependency on translocation of peptide analogs

Taken the cytotoxicity into account, the translocation of the three sCal with the lowest cytotoxicity is investigated. Only Caco-2 tubules with a BI lower than 0.4 were used, to ensure an intact cell barrier. A concentration of 1μM, 1μM and 0.5μM was used of the three analogs sCal(C0,C0), sCal(C4,C4) and sCal(C8,C8), respectively. The location of sCal(C0,C0), sCal(C4,C4) and sCal(C8,C8) is monitored every 40 min over 4 hours using SDCM. Z-stacks of 0.5μm steps are recorded and three positions of interest picked out, these being at the bottom, inside, and above the cells. As seen in figure 21, the analysis of the translocation of the peptide analogs showed no significant difference between sCal(C0,C0) and sCal(C4,C4), which both had constant signals through the 4 hours experiment. Comparing to sCal(C8,C8) a 2 fold increase inside the cells, while

over a 3 fold increase of signal at the bottom of the cells is seen in figure 20. This provides evidence of the sCal(C8,C8) is internalized by the cells and is accumulating at the bottom of the cells. The constant signal at all three locations seen for sCal(C0,C0) and sCal(C4,C4) evince no internalization of these peptide analogs. Since the lipidation increases the hydrophobicity and amphiphilicity, while preserving the overall cationic charge, it is bringing the peptide analogs to gain a cationic cell-penetrating peptide-like effect.[6,18] Though since no translocation of sCal(C0,C0) and sCal(C4,C4) is observed, it could imply that the lipid lengths are too short, therefore not increasing the hydrophobicity and amphiphilicity enough to induce internalization. On the contrary for sCal(C8,C8) the hydrophobicity and amphiphilicity are increased enough, thereby gaining a cationic cell-penetrating peptide-like effect which induces internalization.

The increase in signal of sCal(C8,C8) is steepest between the first two time points, meaning the accumulation happens at the fastest rate in this time slot. After 120 min the slope of the increase starts to flatten out and after 200 min the signal is relatively constant. The accumulation of the peptide, therefore, seems to happen the fastest in the beginning, while over time, less and less peptide gets accumulated at the bottom of the cells. The constant signal at all three locations seen for sCal(C0,C0) and sCal(C4,C4) evince no internalization of these peptide analogs. It is though interesting that the concentration used of sCal(C0,C0) and sCal(C4,C4) is twice the concentration used of sCal(C8,C8), yet no translocation of sCal(C0,C0) and sCal(C4,C4) is seen. This study demonstrates, that introducing lipidation to the sCal peptide could induce peptide translocation across the cell layer, although it is strongly dependent on the length of the lipidations.

After each of the experiments, the BI of the cell tubules is measured again which can be seen in figure 13. The concentrations used in this study are one-fifth for sCal(C0,C0) and sCal(C4,C4) and one-tenth for sCal(C8,C8) of the lowest concentration measured in the LDH cytotoxicity assay. Consistently the BI of the cell tubules is increasing independently of which peptide analog, yet only in a single case, the BI increases slightly above 0.4. This means that even so the BI increases after the experiments, the cell tubule can still be considered intact. The increasing BI questions whether the peptide analogs influence the integrity of the cell barrier or if it is simply the addition of anything else than culture medium. No control experiment investigating this question have been carried out

4.3 Concentration dependency on transport of peptide analogs.

The transport of sCal analogs from the lumen, across the cell barrier, and into the ECM is tracked for approx. 4 hours using WFM. The same concentration of 1μM, 1μM and 0.5μM was used of the same three analogs sCal(C0,C0), sCal(C4,C4) and sCal(C8,C8), respectively. As seen in figure 24a signal of sCal(C0,C0) and sCal(C4,C4) is constant over time, showing no indications of transport to the ECM. This is in good correlation with not seeing any internalization of the peptide previously. However, it is interesting that the signal of sCal(C8,C8) is also constant and neither showing no indications of transport to the ECM. Hence sCal(C8,C8) seems to be internalized and to accumulate beneath the cells, but instead of getting transported to the ECM, sCal(C8,C8) stays beneath the cells. In the previous work done by Trier et al.,[12] acylation of sCal with a single lipidation of C8 increased both membrane binding and uptake of the peptide. In this study, sCal is double lipidated with C8,C8. Accumulation is seen beneath the cells, while no transport is observed. This could indicate that double lipidation of the peptide with C8, induces too strong lipophilicity. This may cause the binding to the membrane to become too strong, making the peptide incapable of releasing the membrane. This would explain the ability to get internalized without being transported to the ECM. Based on these findings there are indications of lipidation itself does not influence the peptides' ability to be internalized by the cells, but the lipid length of the lipidation has to be of a certain length.

Similar to the barrier integrity being measured before and after translocation experiments, the BI was also measured here. However, in this experiment, the transport of TD was tract simultaneously through the entire experiment. A tight control, consisting only of transport medium with TD, is included. This control has increased over time even though no peptide is added, which can be seen in figure 24b. This could be related to what is seen in BI measurements of the translocation study. This gives indications that the BI gets influenced even without the presence of peptides. Through the experiment the TD transport for sCal(C0,C0) and sCal(C4,C4) are constant over time. The TD transport for sCal(C8,C8) does increase over time, yet no significant difference to the control is seen. A control, consisting of a transport medium with TD, of a leaky barrier, is also included, which shows a fold increase of around 550. Comparing to the leaky control, the control and peptide analogs can essentially be considered constant over time.

Since the study of the transport of the peptide analogs shows no transport of neither of the peptide analogs, the concentration of sCal(C0,C0) and sCal(C4,C4) is increased to 10μM to investigate whether the concentration affects the transport. The experiment is carried out as with the lower concentrations as seen in figrue 26a. A fold increase up to 4 and 6 of sCal(C0,C0) and sCal(C4,C4), respectively, is seen. Comparing to the transport seen of the peptides at the lower concentration, a significant difference is observed. However at a concentration of 10μM, no significant difference between sCal(C0,C0) and sCal(C4,C4) was observed. A clear concentration dependency is seen for both sCal(C0,C0) and sCal(C4,C4) as both show high transport at higher concentration. However, at the higher concentration there is no affect of adding the lipidation (going from C0,C0 to C4,C4) as they show the same transport. Importantly sCal(C8,C8) was only tract at low concentration and if possible it would be interesting to see the transport of this peptide analog at high concentration. This was unfortunately not possible due to limitations caused by the low stock concentration due to poor solubility of the peptide analog.

As with the low concentration transport experiment, the transport of TD is monitored over time, which can be seen in figure 26b. Relative to the control, the TD transport for both sCal(C0,C0) and sCal(C4,C4) is lower. Consequently, the peptide analogs do not seem to interfere with the integrity of the cell tubule more than the control of media are able to. Increasing the concentration of the peptide analogs from 1μM to 10μM does not have an effect on the tightness cell barrier. The increase in TD transport seen at both concentrations, which is not significantly higher than the control, could in some manner correlate with the increased BI seen after the translocation experiment.

An important part to consider is the temperature during the transport experiments. In contrast to the study of the translocation of the peptide analogs which is carried out at 37°C, these studies are only performed at room temperature. This is due to it not being practically possible at the time of the experiment. This means that the cell tubule during the 4-hour experiment has experienced a lower temperature than what is suitable for Caco-2 cells. The lowered temperature could possibly influence the cells' ability to internalize and transport the peptide analogs through to the ECM. Speculation on

whether this lowered temperature also can influence the integrity of the cell barrier can also arise. This could be are feasible explanation of the increasing transport of TD over time. It is though still essential to compare to the leaky control of TD transport, which shows a fold increase around 550 while the intact control of TD transport shows a fold increase around 7. Hence the lowered temperature does not interfere with the integrity of the barrier to the extent of it becoming leaky.

5 Conclusion

Double lipidated analogs of sCal, with systematically increasing lipid chain lengths, are investigated using SDCM and WFM. The investigation has been carried out on Caco-2 tubules grown in Mimetas organoplate.

A pierce cytotoxicity assay are performed on sCal(C0,C0), sCal(C4,C4), sCal(C8,C8), sCal(C12,C12) and sCal(C16,C16) and reveal a increased cytotoxicity of for long-chain analogs, chain lengths longer than C4,C4. In addition for the long-chain analogs, a strong concentration dependency was seen on the cytotoxicity. On the contrary, similar cytotoxicity of the negative control, sCal(C0,C0) and sCal(C4,C4) are observed, without any concentration dependency.

translocation of sCal(C0,C0), sCal(C4,C4) and sCal(C8,C8) shows a significant difference between sCal(C0,C0) and sCal(C8,C8) at the bottom of the cells. On the contrary, the analysis showed a strong similarity between sCal(C0,C0) and sCal(C4,C4) with no significant difference. This provides evidence of internalization of sCal(C8,C8) with accumulation below the cells, while no internalization of sCal(C4,C4) takes place.

Transport of sCal(C0,C0) and sCal(C4,C4) at low concentrations, shows no transport of either of the peptide analogs was observed. When increasing the transport of sCal(C0,C0) and sCal(C4,C4) a significant concentration dependency for both was observed and strong evidence of transport is present.

6 Outlook

This study opened numerous new questions about the influence of double lipidation on the internalization and transport of sCal. Two essential hurdles were met during this study. First, the poorly solubility of sCal(C8,C8) caused a low stock concentration. This only allowed a concentration of 0.5μM during the experiments. This also prevented the study of any concentrations dependency on the transport of this peptide analog, which would have been interesting since internalization and accumulation beneath the cells of this peptide analog was seen without actual transport to the ECM. If possible in the future, the study of sCal(C8,C8) at any higher concentration would be very interesting. Second, increasing the temperature to 37°C during the transport experiment is now possible. Investigating whether the temperature increase would influence the transport of the peptide analogs, at both concentrations, would be of great interest. After performing the experiments and data analysis, awareness about measuring the barrier integrity after the transport experiment has emerged. In this way, the BI after the experiment could be quantified and questioning of the integrity of the barrier could be avoided.

To increase the physiological relevance of the system, more complex cell culture of e.g. co-culture of Caco-2 and the mucus secreting HT29-MTX cells can be utilized. In this way, the influence of mucus on the internalization, possible accumulation and transport of the peptide analogs can be elucidated.

The double lipidated library of sCal analogs extend further than the peptide analogs included in this study. sCal with different lipid lengths, e.g. sCal(C4,C8) and sCal(C8,C4), are also available, among others. Expanding the study to also include these sCal analogs would provide further knowledge about the influence of lipidation of peptide drugs.

7 Experimental

7.1 Cell culture

The human adenocarcinoma cell line Caco-2 cells was cultured in T75 flasks in Minimum Essential Medium Eagle from Sigma Aldrich supplemented with 10% fetal bovine serum (FBS), 2% nonessential amino acids (NEAA) and 1% penicillin-streptomycin (P/S).

7.2 LDH assay

A pierce LDH cytotoxicity assay kit is used. The following steps are prepared

- Salmon calcitonin analogs, with C0C0, C4C4, C8C8, C12C12 and C16C16, is diluted to a range of concentrations, 5μM, 10μM, 25μM, 50μM and 75μM, in transportbuffer.
- Dissolve 1 vial of Substrate mix in 11.4 mL ultrapure water
- Reaction mixture: 1 vial of Assay buffer (0.6mL) is diluted in the 11.4 mL Substrate mixture.
- Transport buffer: 10mM habs gelesen buffer pH=6.5

Start by trypsinizing the flask of Caco-2 cells and prepare a stock solution of 5000 cells/well. Transfer 100μL of stock cell solution to a 96-well plate according to the following setup

- sCal(C0,C0) = triplicates of 5 different concentrations = 15 wells
- sCal(C4,C4) = triplicates of 5 different concentrations = 15 wells
- sCal(C8,C8) = triplicates of 5 different concentrations = 15 wells
- sCal(C12,C12) = triplicates of 5 different concentrations = 15 wells
- sCal(C16,C16) = triplicates of 5 different concentrations = 15 wells
- Positive control for max toxicity = 3 wells
- Total number of wells = 78

The plate is incubated for 2 days at 37°C, 5%CO2. After 2 days, add 100μL of each peptide concentration to a appropriate well and incubate for 2 hours at 37°C, 5%CO2. Transfer 50μL of the solution to a new 96-well plate and add 50μL of reaction mixture. Incubate the plate at RT for 30 min protected from light. Measure the absorbance at 490nm and 680nm. To determine LDH activity, subtract the 680nm absorbance value (background) from the 490nm absorbance before calculation of % Cytotoxicity [(LDH at 490nm) - (LDH at 680nm). To calculate % Cytotoxicity, divide the chemical-treated sample LDH activity by the total LDH activity [(Maximum LDH Release Control activity) and multiply by 100.

7.3 Organoplate® culture

This study used 3-lane Organoplates (Mimetas; B4004-404-B) with 400μm x 220μm (w x h) channels. Each observation window was filled with 50μL Hank's balanced salt solution (Hbss) to prevent dehydration and provide optical clarity. 2 μL of ECM mixture, consisting of HEPES:NaHCO3:collagen with a ration of 1:1:8, was dispensed into the gel inlets. After incubation of 35 min at 37°C, 30 cL Hbss was added on top of the gel inlets. The plate was incubated overnight in a humidified incubator at 37°C. CaCo2 cells was trypsinized with 0,25% Trypsin-EDTA solution, aliquoted and pelleted at 200g for 5min. Cell suspension of 1 x 10^7 cells/mL was prepared of CaCo2 cells. 2μL of cell suspension was injected into the inlet of the top medium channel, after which 50 μL of medium was added. The Organoplate®was placed on its side for 3-4 hours at 37°C to allow the cells to attach to the ECM. 50 μL of medium was added to the remaining inlets and outlets of the top and bottom channels. Afterwards, the Organoplate® was placed horizontally in a humidified incubator at 37°C and 5%CO_2 on a interval rocker switching between a +7° and -7° inclination every 8 min allowing biodirectional flow. This results in a flowrate of 2,02 μL/min, giving a sheer stress of 0,13 dyne/cm^2, thereby closely mimicking physiological levels of intestinal epithelial shear stress ranging from 0,002 to 0,08 dyne/cm^2.[66] The medium was refreshed every 2-3 days. 4 days after cells seeding, the plate is ready to use for experiments.

7.4 Immunostaining

Start by preparing the following solutions

- Fixative: 4% paraformaldehyde in Hbss
- Permeabilization buffer: 0.3% Triton X-100
- Blocking solution: 2% FBS, 2% BSA, 0.1% Tween20 in PBS
- Washing solution 4% FBS in PBS
- Antibodies solutions: ZO-1 and Ezrin diluted 1:200

Aspirate medium from chips and add fixative to the inlets and outlets of the chips according to the following table

100μL	0μL	50μL
50μL	0μL	50μL
50μL	0μL	50μL

Table 1: Washing table

Incubate the fixative for 10 min, while the organoplate is placed on a small angle. After 10 min, aspirate the fixative and wash the chips twice (5 min) with PBS according to the table 1. Until otherwise stated, follow the volume scheme in table 1. Wash the chips once in the washing solution for 5 min. Aspirate the washing solution and proceed to permeabilize the cells for 10 min. Wash the chips once in washing solution for 5 min. Aspirate washing solution and add blocking solution. Leave blocking solution in the chips for 45 min. In the meantime prepare appropriate solution of primary antibody in blocking solution. After 45 min, aspirate blocking solution and add primary antibody solution according to the volume scheme in table 2 Leave the antibody solution in for 1 hour at RT placed on a small angle. After 30 min turn the plate.

25μL	0μL	25μL
0μL	0μL	0μL
15μL	0μL	15μL

Table 2: Antibody table

Mean while prepare the secondary antibody solution diluted in blocking solution. After 1 hour aspirate the primary antibody and wash the chips twice for 3 min with

washing solution according to table 1. Then add the secondary antibody solution to the chips according to table 2, place the plate on a small angle in the dark. Leave the secondary antibody in for 1 hour, after 30 min turn the plate. After 1 hour, aspirate the secondary antibody solution and wash the chips twice (3 min) inn washing solution according to table 1. Dilute Dapi stain 1:1000 in PBS and add the solution to the chips for 5 min (in the dark) according to table 1. Lastly wash the chips with PBS three times (5 min).

7.5 Barrier Integrity

Growth media is aspirated from all inlets and outlets. 20μL of fresh growth media is added to gel inlets and outlets and the bottom medium inlets and outlets. 40μL 0.5 mg/ml TRITC-dextran (4.4kDa) is added to the top medium inlets, while 30μL 0.5 mg/ml TRITC-dextran (4.4kDa) is added to the top medium outlets. Afterwards, the Organoplate® was placed horizontally in a humidified incubator for 15 min at 37°C and 5%CO_2 on a interval rocker switching between a +7° and -7° inclination every 8 min. Leakage of TRITC-dextran from the top medium channel into the adjacent gel channel was imaged as a end-point measurement using a spinning disk confocal microscope with 4x objective. The fluorescence intensity profiles and ratios of the fluorescent signal between the two channels were analyzed using ImageJ. A ratio between then top medium channels and the gel channels of <0.3 was accepted as leaktight.

7.6 Internalization study

Growth media is aspirated from all inlets and outlets. 50μL of imaging media, consisting of FluoroBrite with 1% P/S and 2% GlutaMax, is added to gel inlets and outlets along with the bottom medium inlets and outlets. All inlets are washed twice with imaging media. 50μL of staining solution, consisting of CellMask^{TM} Plasma Membrane Stain and Hoechst 33342 diluted in imaging media in a ration of 1:1000 and 1:200, respectively, is added to the top medium inlets and outlets. The Organoplate® is placed horizontally in a humidified incubator for 30 min at 37°C and 5%CO_2 on a interval rocker switching between a +7° and -7° inclination every 8 min. Afterwards, all inlets and outlets are washed twice with imaging media. Peptides solution are prepared with a peptide concentration of 1μM. 100μL of peptide solution is added to the top medium inlet. The peptide

solution is sucked up from the medium outlet and 100μL of peptide solution is added to the top medium inlet. Using a spinning disk confocal microscopy with 60x objective the chips are imaged for 4 hours with a 40min time interval.

7.7 Transport study

Growth media is aspirated from all inlets and outlets. 50μL of imaging media, consisting of FluoroBrite with 1% P/S and 2% GlutaMax, is added to gel inlets and outlets along with the bottom medium inlets and outlets. All inlets are washed twice with imaging media. Peptides solution are prepared with a peptide concentration of 1μM. and TRITC-dextran (4.4kDa) concentration of 0.5 mg/ml. 100μL of peptide solution is added to the top medium inlet. The peptide solution is sucked up from the medium outlet and 100μL of peptide solution is added to the top medium inlet. Using a widefield microscopy with a 10x objective the chips are imaged for 4 hours with a 30s time interval.

7.8 R code

7.8.1 Barrier integrity

```
combined <- read_excel("~/Universitet/Speciale/
Data/Chips/Uptake␣study/BI.xlsx")

std <- function(x) sd(x)/sqrt(length(x))

Data <- summarise(group_by(combined, Treatment),
                  my_mean = mean(BI),
                  my_se = std(BI))


ggplot(Data,aes(x=Treatment,y=my_mean)) +
  theme_classic() +
  ylab("Barrier␣integrity") +
  xlab("sCal␣analogues") +
  scale_y_continuous(limits = c(0,0.5),
  breaks = scales::pretty_breaks(n = 5)) +
```

```
  geom_bar(stat='identity',aes(fill = Treatment)) +
  geom_errorbar(aes(ymin=my_mean-my_se,
  ymax=my_mean+my_se), width=.2, size = 1,
                position = position_dodge(width = 0.8)) +
  scale_fill_brewer(palette = "Set1")  +
  theme(legend.title = element_blank()) +
  theme(legend.position = "none") +
  theme(axis.line = element_line(colour = "black",
                                 size = 2, linetype = "solid"),
        axis.ticks.length=unit(.5, "cm"),
        axis.ticks.x=element_line(size=2),
        axis.ticks.y=element_line(size=2)) +
  geom_point(data = combined,
             aes(y = BI, x = Treatment), size =2) +
  theme(text = element_text(size = 40),
        axis.title.x = element_text(margin = unit(c(5, 0, 0, 0),
        "mm")),
        axis.title.y = element_text(margin = unit(c(0, 5, 0, 0),
        "mm")),
        legend.key.size = unit(3,"line")) +
  geom_vline(xintercept = 1.5,linetype="dashed", size = 2) +
  geom_text(x=3, y=0.48, label="After", size = 12)+
  geom_text(x=1, y=0.48, label="Before", size = 12)
```

7.8.2 Internalization study

7.8.2.1 Extraction of peptide signal as function of time

```
Results <- read_excel("~/Universitet/Speciale/Data/Chips/Uptake
study/Native/20210719/20210719␣area␣1.xlsx")

#Chanel distribution
#  Channel 1: nucleus (Cell mask)
#  Channel 2: peptide (ATTO488)
#  Channel 3: membrane (Hoechst)
```

```
#Dividing the data into each time frame
Frame1 <- Results[1:243,]
Frame2 <- Results[244:486,]
Frame3 <- Results[487:729,]
Frame4 <- Results[730:972,]
Frame5 <- Results[973:1215,]
Frame6 <- Results[1216:1458,]
Frame7 <- Results[1459:1701,]

#Function extracting the membrane signal
Membrane_sig1 <- function(x) x[seq_len(nrow(x)) %% 3 == 0,
seq_len(ncol(x)) %% 5 == 2]

#Extract the membrane signal if each timepoint
Mem_sig_1 <- Membrane_sig1(Frame1)
Mem_sig_2 <- Membrane_sig1(Frame2)
Mem_sig_3 <- Membrane_sig1(Frame3)
Mem_sig_4 <- Membrane_sig1(Frame4)
Mem_sig_5 <- Membrane_sig1(Frame5)
Mem_sig_6 <- Membrane_sig1(Frame6)
Mem_sig_7 <- Membrane_sig1(Frame7)

#Adjusting the membrane signal
Mem_1_adj <- cbind(Mem_sig_1[24:81,])
Mem_2_adj <- cbind(Mem_sig_2[14:71,])
Mem_3_adj <- cbind(Mem_sig_3[7:64,])
Mem_4_adj <- cbind(Mem_sig_4[3:60,])
Mem_5_adj <- cbind(Mem_sig_5[2:59,])
Mem_6_adj <- cbind(Mem_sig_6[2:59,])
Mem_7_adj <- cbind(Mem_sig_7[1:58,])

#Adjusting the membrane intensity
Membrane <- data.frame(Slice = c(1:nrow(Mem_7_adj)),
```

```
                        Time1_0min=rowMeans(Mem_1_adj),
                        Time2_40min=rowMeans(Mem_2_adj),
                        Time3_80min=rowMeans(Mem_3_adj),
                        Time4_120min=rowMeans(Mem_4_adj),
                        Time5_160min=rowMeans(Mem_5_adj),
                        Time6_200min=rowMeans(Mem_6_adj),
                        Time7_240min=rowMeans(Mem_7_adj)) %>%
  gather(key = "TimePoint", value = "Intensity", -Slice)

#standard deviation of membrane signal
Sd_mem <- data.frame(Slice = c(1:nrow(Mem_7_adj)),
                     SD1=apply(Mem_1_adj,1,sd),
                     SD2=apply(Mem_2_adj,1,sd),
                     SD3=apply(Mem_3_adj,1,sd),
                     SD4=apply(Mem_4_adj,1,sd),
                     SD5=apply(Mem_5_adj,1,sd),
                     SD6=apply(Mem_6_adj,1,sd),
                     SD7=apply(Mem_7_adj,1,sd)) %>%
  gather(key = "Frame", value = "SD", -Slice)


#Combine Intensity and standard error to one dataframe
Membrane_sd <- data.frame(Slice = Membrane$Slice, TimePoint =
Membrane$TimePoint, Intensity = Membrane$Intensity, Sd =
Sd_mem$SD)

#Plot membrane intensity as function of microns
ggplot(Peptide_micron, aes(x = Slice/2, y = Intensity, color =
TimePoint)) +
  theme_classic() +
  ylab("Intensity␣[A.U]") +
  theme(legend.title = element_blank()) +
  theme(axis.line = element_line(colour = "black",
                                 size = 2, linetype = "solid"),
```

```
        axis.ticks.length=unit(.5, "cm"),
        axis.ticks.x=element_line(size=2),
        axis.ticks.y=element_line(size=2)) +
  ylab("Intensity␣[A.U]") +
  xlab(expression(paste("Height␣[",mu, m,"]"))) +
  geom_line(size =1)  +
  scale_x_continuous(limits = c(0,30) ,breaks =
  scales::pretty_breaks(n = 10)) +
  scale_y_continuous(breaks = scales::pretty_breaks(n = 5)) +
  scale_color_brewer(palette = "Dark2", labels = c("0␣min","40
␣␣min","80␣min","120␣min","160␣min","200␣min","240␣min"),
  guide = guide_legend(override.aes = list(size = 6, alpha =
  1),reverse=T)) +
  geom_vline(xintercept = c(8,14.5), size = 1) +
  geom_text(x=11, y=140, label="Inside␣cell", color = "black",
  size = 12) +
  geom_text(x=22, y=140, label="Above␣cell", color = "black", size
  = 12) +
  geom_text(x=3, y=140, label="Below␣cell", color = "black", size
  = 12) +
  geom_errorbar(aes(ymin=Intensity-Sd, ymax=Intensity+Sd), alpha =
  0.2, size = 1) +
  theme(text = element_text(size = 40),
        axis.title.x = element_text(margin = unit(c(5, 0, 0, 0),
        "mm")),
        axis.title.y = element_text(margin = unit(c(0, 5, 0, 0),
        "mm")),
        legend.key.size = unit(3,"line"))

#Make combined membrane signal
mmmm<-data.frame(memmean=rowMeans(data.frame(
                          Time1_0min=rowMeans(Mem_1_adj),
                          Time2_40min=rowMeans(Mem_2_adj),
                          Time3_80min=rowMeans(Mem_3_adj),
```

```
                        Time4_120min=rowMeans(Mem_4_adj),
                        Time5_160min=rowMeans(Mem_5_adj),
                        Time6_200min=rowMeans(Mem_6_adj),
                        Time7_240min=rowMeans(Mem_7_adj))),
                    sd=apply(data.frame(Time1_0min=rowMeans(Mem_1_adj
                    ),
                                        Time2_40min=rowMeans(Mem_2_adj),
                                        Time3_80min=rowMeans(Mem_3_adj),
                                        Time4_120min=rowMeans(Mem_4_adj),
                                        Time5_160min=rowMeans(Mem_5_adj),
                                        Time6_200min=rowMeans(Mem_6_adj),
                                        Time7_240min=rowMeans(Mem_7_adj)),
                                        1,sd),
                    Slice=c(1:nrow(Mem_7_adj)))

#Plot combined membrane signal
ggplot(mmmm, aes(x=Slice/2, y=memmean)) +
geom_line() +
theme_bw() +
  theme(plot.title = element_text(hjust = 0.5)) +
  ggtitle("Mean membrane intensity as function of microns from
  13.07")+
  ylab("Membrane mean pixel Intensity [A.U]") +
  xlab(expression(paste("Microns [",mu, m,"]")))  +
  geom_line(size = 1)  +
  scale_x_continuous(breaks = scales::pretty_breaks(n = 10)) +
  scale_y_continuous(breaks = scales::pretty_breaks(n = 10)) +
  scale_color_brewer(palette = "Dark2", guide =
  guide_legend(override.aes
  = list(size = 2, alpha = 1),reverse=T)) +
  geom_vline(xintercept = c(9,13.5)) +
  geom_errorbar(aes(ymin=memmean-sd, ymax=memmean+sd), alpha =
  0.2, size = 1) +
  theme(text = element_text(size = 30))
```

```
#Function extracting the peptide intensities
Peptide_sig1 <- function(x) x[seq_len(nrow(x)) %% 3 == 2,
seq_len(ncol(x)) %% 5 == 2]

#Calculating the mean of the peptide intensity in each timeframe
Pep_sig_1 <- Peptide_sig1(Frame1)
Pep_sig_2 <- Peptide_sig1(Frame2)
Pep_sig_3 <- Peptide_sig1(Frame3)
Pep_sig_4 <- Peptide_sig1(Frame4)
Pep_sig_5 <- Peptide_sig1(Frame5)
Pep_sig_6 <- Peptide_sig1(Frame6)
Pep_sig_7 <- Peptide_sig1(Frame7)

#Adjusting the peptide signal
Pep_1_adj <- Pep_sig_1[24:81,]
Pep_2_adj <- Pep_sig_2[14:71,]
Pep_3_adj <- Pep_sig_3[7:64,]
Pep_4_adj <- Pep_sig_4[3:60,]
Pep_5_adj <- Pep_sig_5[2:59,]
Pep_6_adj <- Pep_sig_6[2:59,]
Pep_7_adj <- Pep_sig_7[1:58,]

#combining the peptide intensity
Peptide <- data.frame(Slice = c(1:nrow(Pep_7_adj)),
                      Time1_0min=rowMeans(Pep_1_adj),
                      Time2_40min=rowMeans(Pep_2_adj),
                      Time3_80min=rowMeans(Pep_3_adj),
                      Time4_120min=rowMeans(Pep_4_adj),
                      Time5_160min=rowMeans(Pep_5_adj),
                      Time6_200min=rowMeans(Pep_6_adj),
                      Time7_240min=rowMeans(Pep_7_adj)) %>%
  gather(key = "TimePoint", value = "Intensity", -Slice)
```

```
#standard deviation of membrane signal
Sd_pep <- data.frame(Slice = c(1:nrow(Pep_7_adj)),
                     SD1=apply(Pep_1_adj,1,sd),
                     SD2=apply(Pep_2_adj,1,sd),
                     SD3=apply(Pep_3_adj,1,sd),
                     SD4=apply(Pep_4_adj,1,sd),
                     SD5=apply(Pep_5_adj,1,sd),
                     SD6=apply(Pep_6_adj,1,sd),
                     SD7=apply(Pep_7_adj,1,sd))%>%
  gather(key = "Frame", value = "SD", -Slice)


#Combine Intensity and SEM to one dataframe
Peptide_micron <- data.frame(Slice = Peptide$Slice, TimePoint =
Peptide$TimePoint, Intensity = Peptide$Intensity, Sd = Sd_pep$SD)

#plotting the pepitde signal as function of microns
ggplot(Peptide_micron, aes(x = Slice/2, y = Intensity,
color = TimePoint)) +
  theme_bw() +
  ggtitle("Peptide␣signal␣for␣sCal(C0/C0)-ATTO488") +
  theme(plot.title = element_text(hjust = 0.5)) +
  ylab("Peptide␣mean␣pixel␣Intensity␣[A.U]") +
  xlab(expression(paste("Microns␣[",mu, m,"]"))) +
  geom_line(size = 1) +
  scale_x_continuous(breaks = scales::pretty_breaks(n = 10)) +
  scale_y_continuous(breaks = scales::pretty_breaks(n = 10)) +
  scale_color_brewer(palette = "Dark2", guide =
  guide_legend(override.aes
  = list(size = 2, alpha = 1),reverse=T)) +
  geom_vline(xintercept = c(9,13.5))+
  geom_text(x=12.5, y=135, label="<-Inside␣cell->", color = "red",
  size = 8) +
  geom_errorbar(aes(ymin=Intensity-Sd, ymax=Intensity+Sd),
```

```
  alpha =0.2, size = 1) +
  theme(text = element_text(size = 30))

Bottom <- 18
Inside <- 25
Top <- 41
#Extracting the peptide intensity increasing over time for certain
microns
Location_intensity <- data.frame(Bottom =
Peptide_micron$Intensity[Peptide_micron$Slice==Bottom],
Inside = Peptide_micron$Intensity[Peptide_micron$Slice==Inside],
Top = Peptide_micron$Intensity[Peptide_micron$Slice==Top],
TimePoint = c(0,40,80,120,160,200,240)) %>%
  gather(key = "Location", value = "Intensity", -TimePoint)

sd_micron <- data.frame(Bottom = Sd_pep$SD[Sd_pep$Slice==Bottom],
                        Inside = Sd_pep$SD[Sd_pep$Slice==Inside],
                        Top = Sd_pep$SD[Sd_pep$Slice==Top]) %>%
  gather(key = "Location", value = "SD")


Intensity_over_time <- data.frame(Location_intensity, Sd =
sd_micron$SD)

ggplot(Intensity_over_time, aes(x=TimePoint, y=Intensity,
color = Location)) +
  theme_bw() +
  ggtitle("Peptide␣signal␣as␣function␣of␣time␣for
␣␣sCal(C0/C0)-ATTO488") +
  theme(plot.title = element_text(hjust = 0.5))+
  ylab("Peptide␣mean␣pixel␣Intensity␣[A.U]") +
  xlab("Time␣[min]")  +
  geom_line(size = 1)+
  geom_point()+
```

```
  scale_x_continuous(breaks = scales::pretty_breaks(n = 7)) +
  scale_y_continuous(breaks = scales::pretty_breaks(n = 10)) +
  scale_color_brewer(palette = "Set1", guide =
  guide_legend(override.aes
  = list(size = 2, alpha = 1))) +
  geom_errorbar(aes(ymin=Intensity-Sd, ymax=Intensity+Sd),
  width=.2,position=position_dodge(0.05), alpha = 0.5, size =1) +
  theme(text = element_text(size = 30))
```

7.8.2.2 Plotting of peptide signal as function of time for individual peptides

```
data <- data.frame(data_20210702$Intensity,
data_20210717$Intensity,
data_20210719$Intensity)-100

std <- function(x) sd(x)/sqrt(length(x))

Collected <- data.frame(Timepoint = data_20210702$TimePoint,
Location = data_20210702$Location,
Intensity = rowMeans(data), SEM = apply(data,1,std))

norm <- rep(c(Collected$Intensity[1],
Collected$Intensity[8],
Collected$Intensity[15]), each = 7)

Final<-data.frame(Timepoint = Collected$Timepoint,
Location = Collected$Location,
Intensity = Collected$Intensity/norm,
SEM = Collected$SEM/norm)

ggplot(Final, aes(x=Timepoint, y=Intensity, color = Location)) +
  theme_classic() +
  theme(legend.title = element_blank()) +
```

```
  theme(axis.line = element_line(colour = "black",
                                 size = 2, linetype = "solid"),
        axis.ticks.length=unit(.5, "cm"),
        axis.ticks.x=element_line(size=2),
        axis.ticks.y=element_line(size=2)) +
  ylab("Realative␣Internalization") +
  xlab("Time␣[min]") +
  geom_point(size = 5)+
  geom_line() +
  scale_x_continuous(breaks = scales::pretty_breaks(n = 7)) +
  scale_y_continuous(breaks = scales::pretty_breaks(n = 10)) +
  scale_color_brewer(palette = "Set1",
  labels = c("Below","Inside","Above"),
  guide = guide_legend(override.aes = list(size = 6,
  alpha = 1),reverse = T)) +
  geom_errorbar(aes(ymin=Intensity-SEM, ymax=Intensity+SEM),
  width=.2, position=position_dodge(0.05), alpha = 0.5, size =1) +
  theme(text = element_text(size = 40),
  axis.title.x = element_text(margin = unit(c(5, 0, 0, 0), "mm")),
  axis.title.y = element_text(margin = unit(c(0, 5, 0, 0), "mm")),
  legend.key.size = unit(3,"line"))
```

7.8.2.3 Combining data from individual peptides into a single plot

```
#C0C0
data_20210702 <- read_excel("~/Universitet/Speciale/Data/Chips
/Uptake␣study/Native/20210702/20210702␣Intensity␣over␣time.xlsx")
data_20210717 <- read_excel("~/Universitet/Speciale/Data/Chips
/Uptake␣study/Native/20210717/20210717␣Intensity␣over␣time.xlsx")
data_20210719 <- read_excel("~/Universitet/Speciale/Data/Chips
/Uptake␣study/Native/20210719/20210719␣Intensity␣over␣time.xlsx")

#C4C4
data_20210706 <- read_excel("~/Universitet/Speciale/Data/Chips
```

```
/Uptake␣study/C4/20210706/20210706␣Intensity␣over␣time.xlsx")
data_20210713 <- read_excel("~/Universitet/Speciale/Data/Chips
/Uptake␣study/C4/20210713/20210713␣Intensity␣over␣time.xlsx")
data_20210716 <- read_excel("~/Universitet/Speciale/Data/Chips
/Uptake␣study/C4/20210716/20210716␣Intensity␣over␣time.xlsx")

#C8C8
data_20210216 <- read_excel("~/Universitet/Speciale/Data/Chips
/Uptake␣study/C8/20210216/20210216␣Intensity␣over␣time.xlsx")
data_20210708 <- read_excel("~/Universitet/Speciale/Data/Chips
/Uptake␣study/C8/20210708/20210708␣Intensity␣over␣time.xlsx")
data_20210711 <- read_excel("~/Universitet/Speciale/Data/Chips
/Uptake␣study/C8/20210711/20210711␣Intensity␣over␣time.xlsx")

data_C8C8 <- data.frame(data_20210216$Intensity,
data_20210708$Intensity,data_20210711$Intensity)-autoflurescence

data_C4C4 <- data.frame(data_20210706$Intensity,
data_20210713$Intensity,data_20210716$Intensity)-autoflurescence

data_C0C0 <- data.frame(data_20210702$Intensity,
data_20210717$Intensity, data_20210719$Intensity)-autoflurescence

C8 <- rowMeans(data_C8C8)
C4 <- rowMeans(data_C4C4)
C0 <- rowMeans(data_C0C0)


std <- function(x) sd(x)/sqrt(length(x))

SEM_C8C8 <- apply(data_C8C8,1,std)/C8[1]
SEM_C4C4 <- apply(data_C4C4,1,std)/C4[1]
SEM_C0C0 <- apply(data_C0C0,1,std)/C0[1]
```

```
Collected <- data.frame(Timepoint = data_20210216$TimePoint,
            Location = data_20210216$Location,
            Intensity = c(C8/C8[1],C4/C4[1],C0/C0[1]),
            SEM = c(SEM_C8C8,SEM_C4C4,SEM_C0C0),
            Treatment = rep(c("C8,C8","C4,C4","C0,C0"), each = 21))
            %>%
  filter(Location == "Below")

ggplot(Collected, aes(x=Timepoint, y=Intensity, color =
Treatment)) +
  theme_classic() +
  theme(legend.title = element_blank()) +
  theme(axis.line = element_line(colour = "black",
                                 size = 2, linetype = "solid"),
        axis.ticks.length=unit(.5, "cm"),
        axis.ticks.x=element_line(size=2),
        axis.ticks.y=element_line(size=2)) +
  ylab("Relative␣Internalization") +
  xlab("Time␣[min]") +
  geom_point(size = 5)+
  geom_line(size = 1) +
  scale_x_continuous(breaks = scales::pretty_breaks(n = 7)) +
  scale_y_continuous(breaks = scales::pretty_breaks(n = 5)) +
  scale_color_brewer(palette = "Set1",
  guide = guide_legend(override.aes = list(size = 6,
  alpha =1),reverse = T)) +
  geom_errorbar(aes(ymin=Intensity-SEM, ymax=Intensity+SEM),
  width=.2, position=position_dodge(0.05), alpha = 0.5, size =1) +
  theme(text = element_text(size = 40),
  axis.title.x = element_text(margin = unit(c(5, 0, 0, 0), "mm")),
  axis.title.y = element_text(margin = unit(c(0, 5, 0, 0), "mm")),
  legend.key.size = unit(3,"line"))
```

```
#barplot
barplot <- read_excel("~/Universitet/Speciale/Data/
Chips/Uptake␣study/barplot.xlsx")

t.test(barplot$Intensity[barplot$Condition == "C0,C0"],
       barplot$Intensity[barplot$Condition == "C4,C4"])$p.value
t.test(barplot$Intensity[barplot$Condition == "C0,C0"],
       barplot$Intensity[barplot$Condition == "C8,C8"])$p.value

Comparison <- summarise(group_by(barplot, Condition),
                        my_mean = mean(Intensity),
                        my_se = std(Intensity))
data_C8C8[1,]

ggplot(Comparison,aes(x=Condition,y=my_mean)) +
  theme_classic() +
  ylab("Relative␣Internalization") +
  theme(legend.title = element_blank()) +
  theme(axis.line = element_line(colour = "black",
                                 size = 2, linetype = "solid"),
        axis.ticks.length=unit(.5, "cm"),
        axis.ticks.x=element_line(size=2),
        axis.ticks.y=element_line(size=2)) +
  geom_bar(stat="identity", width=.5, fill = "#56B4E9") +
  geom_errorbar(aes(ymin=my_mean-my_se, ymax=my_mean+my_se),
  width=.2, size = 1,
  position = position_dodge(width = 0.5)) +
  scale_fill_brewer(palette = "Set1",
  labels = c("1␣uM", "10␣uM")) +
  geom_point(data = barplot,
             aes(y = Intensity, x = Condition),
             position = position_dodge(width = .5), size = 3) +
  geom_signif(stat="identity",
              data=data.frame(x=c(3, 1), xend=c(1.0, 2.0),
```

```
                y=c(4.2, 4), annotation=c("*", "NS")),
                aes(x=x,xend=xend, y=y, yend=y,
                annotation=annotation,
                textsize = 10), tip_length = 1) +
  theme(text = element_text(size = 40),
        axis.title.x = element_text(margin =
        unit(c(5, 0, 0, 0), "mm")),
        axis.title.y = element_text(margin =
        unit(c(0, 5, 0, 0), "mm")),
        legend.key.size = unit(3,"line"))
```

7.8.3 Transport study

7.8.3.1 Extraction peptide and dextran signal for each individual peptide

```
ecm_20210618 <- read_excel("~/Universitet/Speciale/Data/Chips
/Transport␣study/20210618/20210618␣ecm.xlsx")
cell_20210618 <- read_excel("~/Universitet/Speciale/Data/Chips
/Transport␣study/20210618/20210618␣cell.xlsx")

ecm_20210521 <- read_excel("~/Universitet/Speciale/Data/Chips
/Transport␣study/20210521/20210521␣ecm.xlsx")
cell_20210521 <- read_excel("~/Universitet/Speciale/Data/Chips
/Transport␣study/20210521/20210521␣cell.xlsx")

Data_20210521 = data.frame(ECM_lane = ecm_20210521$Mean1,
                           Cell_lane = cell_20210521$Mean1,
                           Treatment = rep(c("non","Control",
                           "C4C4␣1␣uM", "C0C0␣10␣uM"), each = 2),
                           Channel = c("Peptide","Dextran"),
                           Time =rep(seq(0,14040,30), each = 8))

Data_20210618 = data.frame(ECM_lane = ecm_20210618$Mean1,
                         Cell_lane = cell_20210618$Mean1,
```

```
                        Treatment = rep(c("Control","C0C0␣1",
                        "C0C0␣2", "C0C0␣3", "C4C4", "C8C8"),
                        each = 2),
                        Channel = c("Peptide","Dextran"),
                        Time =rep(seq(0,14490,45), each = 12))

Collected_20210618  <- filter(Data_20210618,Time %in%
Data_20210521$Time)
Collected_20210521  <- filter(Data_20210521,Time %in%
Data_20210618$Time)


Peptide_C0C0_1 <- Collected_20210618 %>%
  slice(which(row_number() %% 12 == 3 ))

Dextran_C0C0_1 <- Collected_20210618 %>%
  slice(which(row_number() %% 12 == 4))

Peptide_C0C0_2 <- Collected_20210618 %>%
  slice(which(row_number() %% 12 == 5 ))

Dextran_C0C0_2 <- Collected_20210618 %>%
  slice(which(row_number() %% 12 == 6))

Peptide_C0C0_3 <- Collected_20210618 %>%
  slice(which(row_number() %% 12 == 7 ))

Dextran_C0C0_3 <- Collected_20210618 %>%
  slice(which(row_number() %% 12 == 8))

PE <- data.frame(C0C0_1 =
Peptide_C0C0_1$ECM_lane-mean(Peptide_C0C0_1$ECM_lane[1:3]),
                          C0C0_2 = Peptide_C0C0_2$ECM_lane-
                          mean(Peptide_C0C0_2$ECM_lane[1:3]),
```

```
                          C0C0_3 = Peptide_C0C0_3$ECM_lane-
                          mean(Peptide_C0C0_3$ECM_lane[1:3]))

Peptide_ecm <- data.frame(mapply('/',PE,PE[4,]))

PC <- data.frame(C0C0_1 =
Peptide_C0C0_1$Cell_lane-mean(Peptide_C0C0_1$Cell_lane[1:3]),
                           C0C0_2 = Peptide_C0C0_2$Cell_lane-
                           mean(Peptide_C0C0_2$Cell_lane[1:3]),
                           C0C0_3 = Peptide_C0C0_3$Cell_lane-
                           mean(Peptide_C0C0_3$Cell_lane[1:3]))

Peptide_cell<- data.frame(mapply('/',PC,PC[4,]))

DE <- data.frame(C0C0_1 =
Dextran_C0C0_1$ECM_lane-mean(Dextran_C0C0_1$ECM_lane[1:3]),
                          C0C0_2 = Dextran_C0C0_2$ECM_lane-
                          mean(Dextran_C0C0_2$ECM_lane[1:3]),
                          C0C0_3 = Dextran_C0C0_3$ECM_lane-
                          mean(Dextran_C0C0_3$ECM_lane[1:3]))

Dextran_ecm<- data.frame(mapply('/',DE,DE[4,]))

DC <- data.frame(C0C0_1 =
Dextran_C0C0_1$Cell_lane-mean(Dextran_C0C0_1$Cell_lane[1:3]),
                           C0C0_2 = Dextran_C0C0_2$Cell_lane-
                           mean(Dextran_C0C0_2$Cell_lane[1:3]),
                           C0C0_3 = Dextran_C0C0_3$Cell_lane-
                           mean(Dextran_C0C0_3$Cell_lane[1:3]))

Dextran_cell<- data.frame(mapply('/',DC,DC[4,]))

SEM <- function(x) sd(x)/sqrt(length(x))
```

```
Collected <- data.frame(ECM_lane =
c(rowMeans(Peptide_ecm[4:nrow(Peptide_ecm),]),
rowMeans(Dextran_ecm[4:nrow(Dextran_ecm),])),
Cell_lane = c(rowMeans(Peptide_cell[4:nrow(Peptide_cell),]),
rowMeans(Dextran_cell[4:nrow(Dextran_cell),])),
                        Time =rep(seq(0,13770,90), times = 2),
                        Channel = rep(c("Peptide","Dextran"),
                        each = nrow(Peptide_ecm)-3)) %>%
  gather(key = "Lane", value = "Intensity", -Channel, -Time)

DATA <- data.frame(Collected, SEM =
c(apply(Peptide_ecm[4:nrow(Peptide_ecm),],1,SEM),
apply(Dextran_ecm[4:nrow(Dextran_ecm),],1,SEM),
apply(Peptide_cell[4:nrow(Peptide_cell),],1,SEM),
apply(Dextran_cell[4:nrow(Dextran_cell),],1,SEM)))

ggplot(DATA, aes(x = Time/60, y = Intensity, color= Channel)) +
  geom_line(size=1) +
  theme_bw() +
  ggtitle("sCal(C0C0)-ATTO488␣1␣uM,␣n=3") +
  theme(plot.title = element_text(hjust = 0.5)) +
  ylab("Intensity␣[A.U]") +
  xlab(expression(paste("Time␣[min]"))) +
  geom_line(size =1) +
  scale_x_continuous(breaks = scales::pretty_breaks(n = 5)) +
  scale_y_continuous(breaks = scales::pretty_breaks(n =
  5),sec.axis = sec_axis(~. /40)) +
  scale_color_brewer(palette = "Set1",
  guide = guide_legend(override.aes = list(size = 6, alpha =
  1),reverse=T)) +
  geom_errorbar(aes(ymin=Intensity-SEM,
  ymax=Intensity+SEM), alpha = 0.2, size = 1) +
  facet_wrap(~Lane) +
  theme(text = element_text(size = 40))
```

7.8.3.2 Combined plotting of transport data

```
Data_1_peptide<-data.frame(bind_rows(C0C0_1,C4C4_1,C8C8_1,dextran
Condition = rep(c("sCT(C0,C0)","sCT(C4,C4)","sCT(C8,C8)",
"Control"), each = 308)) %>%
  filter(Channel == "Peptide")
Data_1_dextran<-data.frame(bind_rows(C0C0_1,C4C4_1,C8C8_1,dextran
Condition = rep(c("sCT(C0,C0)","sCT(C4,C4)","sCT(C8,C8)",
"Control"), each = 308)) %>%
  filter(Channel == "Dextran") %>%
  bind_rows(pos_dex) %>%
  mutate(condition = rep(c("B","C","D", "A","E"), each = 154))

ggplot(Data_1_peptide, aes(x = Time/60, y = Intensity, color=
Condition)) +
  geom_line(size=1) +
  theme_classic() +
  theme(legend.title = element_blank()) +
  theme(axis.line = element_line(colour = "black",
                                 size = 2, linetype = "solid"),
        axis.ticks.length=unit(.5, "cm"),
        axis.ticks.x=element_line(size=2),
        axis.ticks.y=element_line(size=2)) +
  ylab("Relative␣transport") +
  xlab(expression(paste("Time␣[min]"))) +
  scale_x_continuous(limits = c(0,240),breaks =
  scales::pretty_breaks(n = 5)) +
  scale_y_continuous(breaks = scales::pretty_breaks(n = 10)) +
  scale_color_brewer(palette = "Set1", labels =
  c("Control","C0,C0","C4,C4","C8,C8"),
  guide = guide_legend(override.aes = list(size = 6, alpha =
  1),reverse=T)) +
  geom_errorbar(aes(ymin=Intensity-SEM, ymax=Intensity+SEM), alpha
  = 0.5, size = 0.5) +
```

```
  theme(text = element_text(size = 40),
        axis.title.x = element_text(margin = unit(c(5, 0, 0, 0),
        "mm")),
        axis.title.y = element_text(margin = unit(c(0, 5, 0, 0),
        "mm")),
        legend.key.size = unit(3,"line"))

ggplot(Data_1_dextran, aes(x = Time/60, y = Intensity,
color= condition)) +
  geom_line(size=1) +
  theme_classic() +
  theme(legend.title = element_blank()) +
  theme(axis.line = element_line(colour = "black",
                                 size = 2, linetype = "solid"),
        axis.ticks.length=unit(.5, "cm"),
        axis.ticks.x=element_line(size=2),
        axis.ticks.y=element_line(size=2)) +
  ylab("Relative␣transport") +
  xlab(expression(paste("Time␣[min]"))) +
  scale_x_continuous(limits = c(0,240),breaks =
  scales::pretty_breaks(n = 5)) +
  scale_y_continuous(breaks = scales::pretty_breaks(n = 10)) +
  scale_color_brewer(palette = "Set1", labels =
  c("Control","C0,C0","C4,C4","C8,C8","Leaky␣Control"),
  guide = guide_legend(override.aes = list(size = 6, alpha =
  1),reverse=T)) +
  geom_errorbar(aes(ymin=Intensity-SEM, ymax=Intensity+SEM),
  alpha = 0.5, size = 0.5) +
  theme(text = element_text(size = 40),
        axis.title.x = element_text(margin = unit(c(5, 0, 0, 0),
        "mm")),
        axis.title.y = element_text(margin = unit(c(0, 5, 0, 0),
        "mm")),
        legend.key.size = unit(3,"line")) +
```

```
  facet_zoom(ylim = c(-15, 15))

#Data with 10 uM
Data_10_peptide<-data.frame(rbind(C0C0_10,C4C4_10,dextran),
Condition = rep(c("sCT(C0,C0)","sCT(C4,C4)","Control"), each =
308)) %>%
  filter(Channel == "Peptide")
Data_10_dextran<-data.frame(rbind(C0C0_10,C4C4_10,dextran),
Condition = rep(c("sCT(C0,C0)","sCT(C4,C4)","Control"), each =
308)) %>%
  filter(Channel == "Dextran")

ggplot(Data_10_peptide, aes(x = Time/60, y = Intensity, color=
Condition)) +
  geom_line(size=1) +
  theme_classic() +
  theme(legend.title = element_blank()) +
  theme(axis.line = element_line(colour = "black",
                                 size = 2, linetype = "solid"),
        axis.ticks.length=unit(.5, "cm"),
        axis.ticks.x=element_line(size=2),
        axis.ticks.y=element_line(size=2)) +
  ylab("Relative␣transport") +
  xlab(expression(paste("Time␣[min]"))) +
  scale_x_continuous(limits = c(0,240),breaks =
  scales::pretty_breaks(n = 5)) +
  scale_y_continuous(limits = c(0,8),breaks =
  scales::pretty_breaks(n = 10)) +
  scale_color_brewer(palette = "Set1", labels =
  c("Control","C0,C0","C4,C4"),
  guide = guide_legend(override.aes = list(size = 6, alpha =
  1),reverse=T)) +
  geom_errorbar(aes(ymin=Intensity-SEM, ymax=Intensity+SEM), alpha
  = 0.5, size = 0.5) +
```

```
  theme(text = element_text(size = 40),
        axis.title.x = element_text(margin = unit(c(5, 0, 0, 0),
        "mm")),
        axis.title.y = element_text(margin = unit(c(0, 5, 0, 0),
        "mm")),
        legend.key.size = unit(3,"line"))

ggplot(Data_10_dextran, aes(x = Time/60, y = Intensity, color=
Condition)) +
  geom_line(size=1) +
  theme_classic() +
  theme(legend.title = element_blank()) +
  theme(axis.line = element_line(colour = "black",
                                 size = 2, linetype = "solid"),
        axis.ticks.length=unit(.5, "cm"),
        axis.ticks.x=element_line(size=2),
        axis.ticks.y=element_line(size=2)) +
  ylab("Intensity␣[A.U]") +
  xlab(expression(paste("Time␣[min]"))) +
  scale_x_continuous(limits = c(0,240),breaks =
  scales::pretty_breaks(n = 5)) +
  scale_y_continuous(limits = c(0,9),breaks =
  scales::pretty_breaks(n = 10)) +
  scale_color_brewer(palette = "Set1", labels =
  c("Control","C0,C0","C4,C4"),
  guide = guide_legend(override.aes = list(size = 6, alpha =
  1),reverse=T)) +
  geom_errorbar(aes(ymin=Intensity-SEM, ymax=Intensity+SEM), alpha
  = 0.5, size = 0.5) +
  theme(text = element_text(size = 40),
        axis.title.x = element_text(margin = unit(c(5, 0, 0, 0),
        "mm")),
        axis.title.y = element_text(margin = unit(c(0, 5, 0, 0),
        "mm")),
```

```
        legend.key.size = unit(3,"line"))

#Combined

Data_peptide <- data.frame(rbind(C0C0_1,C4C4_1,C8C8_1,C0C0_10,
C4C4_10,dextran),
Condition = rep(c("sCT(C0,C0) 1 uM",
"sCT(C4,C4) 1 uM","sCT(C8,C8) 1uM",
"sCT(C0,C0) 10 uM","sCT(C4,C4) 10uM",
"Control"), each = 308)) %>%
  filter(Channel == "Peptide")
Data_dextran <- data.frame(rbind(C0C0_1,C4C4_1,C8C8_1,C0C0_10,
C4C4_10,dextran), Condition = rep(c("sCT(C0,C0) 1 uM",
"sCT(C4,C4) 1 uM","sCT(C8,C8) 1 uM",
"sCT(C0,C0) 10 uM","sCT(C4,C4) 10 uM",
"Control"), each = 308)) %>%
  filter(Channel == "Dextran")

ggplot(Data_peptide, aes(x = Time/60, y = Intensity, color=
Condition)) +
  geom_line(size=1) +
  theme_classic() +
  theme(legend.title = element_blank()) +
  theme(axis.line = element_line(colour = "black",
                                 size = 2, linetype = "solid"),
        axis.ticks.length=unit(.5, "cm"),
        axis.ticks.x=element_line(size=2),
        axis.ticks.y=element_line(size=2)) +
  ylab("Relative transport") +
  xlab(expression(paste("Time [min]"))) +
  scale_x_continuous(limits = c(0,240),breaks =
  scales::pretty_breaks(n = 5)) +
  scale_y_continuous(limits = c(-2,8),breaks =
  scales::pretty_breaks(n = 10)) +
```

```
  scale_color_brewer(palette = "Set1", labels =
  c("Control","C0,C0␣1uM","C0,C0␣10uM","C4,C4␣1uM",
  "C4,C4␣10uM","C8,C8␣1uM"),
  guide = guide_legend(override.aes =
  list(size = 6, alpha = 1),reverse=T)) +
  geom_errorbar(aes(ymin=Intensity-SEM, ymax=Intensity+SEM),
  alpha = 0.5, size = 0.5) +
  theme(text = element_text(size = 40),
        axis.title.x = element_text(margin = unit(c(5, 0, 0, 0),
        "mm")),
        axis.title.y = element_text(margin = unit(c(0, 5, 0, 0),
        "mm")),
        legend.key.size = unit(3,"line"))

ggplot(Data_dextran, aes(x = Time/60, y = Intensity, color=
Condition)) +
  geom_line(size=1) +
  theme_classic() +
  theme(legend.title = element_blank()) +
  theme(axis.line = element_line(colour = "black",
                                 size = 2, linetype = "solid"),
        axis.ticks.length=unit(.5, "cm"),
        axis.ticks.x=element_line(size=2),
        axis.ticks.y=element_line(size=2)) +
  ylab("Relative␣transport") +
  xlab(expression(paste("Time␣[min]"))) +
  scale_x_continuous(limits = c(0,240),breaks =
  scales::pretty_breaks(n = 5)) +
  scale_y_continuous(breaks = scales::pretty_breaks(n = 10)) +
  scale_color_brewer(palette = "Set1", labels = c("Control","C0,C0
␣␣1␣uM","C0,C0␣10␣uM","C4,C4␣1␣uM","C4,C4␣10␣uM","C8,C8␣1␣uM"),
                     guide = guide_legend(override.aes =
                     list(size=6, alpha = 1),reverse=T)) +
  geom_errorbar(aes(ymin=Intensity-SEM, ymax=Intensity+SEM), alpha
```

```
  = 0.5, size = 0.5) +
  theme(text = element_text(size = 40),
        axis.title.x = element_text(margin = unit(c(5, 0, 0, 0),
        "mm")),
        axis.title.y = element_text(margin = unit(c(0, 5, 0, 0),
        "mm")),
        legend.key.size = unit(3,"line"))


#Barplot
barplot <- read_excel("~/Universitet/Speciale/Data/Chips/
Transport␣study/collected␣barplot.xlsx")


t.test(barplot$Intensity[barplot$Condition == "C0,C0" &
barplot$Concentration == "A"],
       barplot$Intensity[barplot$Condition == "C0,C0" &
       barplot$Concentration == "B"])$p.value

t.test(barplot$Intensity[barplot$Condition == "C4,C4" &
barplot$Concentration == "A"],
       barplot$Intensity[barplot$Condition == "C4,C4" &
       barplot$Concentration == "B"])$p.value

t.test(barplot$Intensity[barplot$Condition == "C0,C0" &
barplot$Concentration == "A"],
       barplot$Intensity[barplot$Condition == "C4,C4" &
       barplot$Concentration == "A"])$p.value

t.test(barplot$Intensity[barplot$Condition == "C0,C0" &
barplot$Concentration == "A"],
       barplot$Intensity[barplot$Condition == "C8,C8" &
       barplot$Concentration == "A"])$p.value
```

```
t.test(barplot$Intensity[barplot$Condition == "C0,C0" &
barplot$Concentration == "B"],
       barplot$Intensity[barplot$Condition == "C4,C4" &
       barplot$Concentration == "B"])$p.value



std <- function(x) sd(x)/sqrt(length(x))

Comparison <- summarise(group_by(barplot, Condition,
Concentration),
                  my_mean = mean(Intensity),
                  my_se = std(Intensity))


ggplot(Comparison,aes(x=Condition,y=my_mean)) +
  theme_classic() +
  ylab("Relative␣transport") +
  theme(legend.title = element_blank()) +
  theme(axis.line = element_line(colour = "black",
                                 size = 2, linetype = "solid"),
        axis.ticks.length=unit(.5, "cm"),
        axis.ticks.x=element_line(size=2),
        axis.ticks.y=element_line(size=2)) +
  scale_y_continuous(limits = c(-2,9),breaks =
  scales::pretty_breaks(n = 9)) +
  geom_bar(aes(fill = Concentration), stat="identity",
  position="dodge", width=.5) +
  geom_errorbar(aes(ymin=my_mean-my_se, ymax=my_mean+my_se, group
  = Concentration),  width=.2, size = 1,
                position = position_dodge(width = 0.5)) +
  scale_fill_brewer(palette = "Set1", labels = c("1␣uM", "10␣uM"))
  +
  geom_point(data = barplot,
```

```
            aes(y = Intensity, x = Condition, fill =
            Concentration),
            position = position_dodge(width = .5), size = 3) +
geom_signif(stat="identity",
             data=data.frame(x=c(0.875, 1.875), xend=c(1.125,
             2.125),
                             y=c(5.8, 8.5), annotation=c("**",
                             "*")),
             aes(x=x,xend=xend, y=y, yend=y,
             annotation=annotation, textsize = 10)) +
theme(text = element_text(size = 40),
      axis.title.x = element_text(margin = unit(c(5, 0, 0, 0),
      "mm")),
      axis.title.y = element_text(margin = unit(c(0, 5, 0, 0),
      "mm")),
      legend.key.size = unit(3,"line"))
```

References

[1] S. Mitragotri, P. A. Burke and R. Langer, *Nature Reviews Drug Discovery*, 2014, **13**, 655–672.

[2] D. J. Drucker, *Nature Reviews Drug Discovery*, 2020, **19**, 277–289.

[3] P. Li, H. M. Nielsen and A. Müllertz, *Expert Opinion on Drug Delivery*, 2012, **9**, 1289–1304.

[4] P. Tyagi, S. Pechenov and J. Anand Subramony, *Journal of Controlled Release*, 2018, **287**, 167–176.

[5] M. Kristensen and H. M. Nielsen, *Tissue Barriers*, 2016, **4**, —.

[6] J. Renukuntla, A. D. Vadlapudi, A. Patel, S. H. Boddu and A. K. Mitra, *International Journal of Pharmaceutics*, 2013, **447**, 75–93.

[7] A. F. B. Räder, M. Weinmüller, F. Reichart, A. Schumacher-Klinger, S. Merzbach, C. Gilon, A. Hoffman and H. Kessler, *Angewandte Chemie*, 2018, **130**, 14614–14640.

[8] N. Tsomaia, *European Journal of Medicinal Chemistry*, 2015, **94**, 459–470.

[9] M. A, S. F, J. MA, A. M, M. N, J. GK, W. MH and A. FJ, *Saudi pharmaceutical journal : SPJ : the official publication of the Saudi Pharmaceutical Society*, 2016, **24**, 413–428.

[10] B. F. Choonara, Y. E. Choonara, P. Kumar, D. Bijukumar, L. C. du Toit and V. Pillay, *Biotechnology Advances*, 2014, **32**, 1269–1282.

[11] R. Menacho-Melgar, J. S. Decker, J. N. Hennigan and M. D. Lynch, *Journal of Controlled Release*, 2019, **295**, 1–12.

[12] S. Trier, L. Linderoth, S. Bjerregaard, H. M. Strauss, U. L. Rahbek and T. L. Andresen, *European Journal of Pharmaceutics and Biopharmaceutics*, 2015, **96**, 329–337.

[13] P. Lundquist and P. Artursson, *Advanced Drug Delivery Reviews*, 2016, **106**, 256–276.

[14] C. Beaurivage, E. Naumovska, Y. X. Chang, E. D. Elstak, A. Nicolas, H. Wouters, G. van Moolenbroek, H. L. Lanz, S. J. Trietsch, J. Joore, P. Vulto, R. A. Janssen, K. S. Erdmann, J. Stallen and D. Kurek, *International Journal of Molecular Sciences*, 2019, **20**, —.

[15] B. Zhang, A. Korolj, B. F. L. Lai and M. Radisic, *Nature Reviews Materials 2018 3:8*, 2018, **3**, 257–278.

[16] C. A. M. Fois, T. Y. L. Le, A. Schindeler, S. Naficy, D. D. McClure, M. N. Read, P. Valtchev, A. Khademhosseini and F. Dehghani, *Advanced Healthcare Materials*, 2019, **8**, —.

[17] B. Zhang and M. Radisic, *Lab on a Chip*, 2017, **17**, 2395–2420.

[18] W. B. Kauffman, T. Fuselier, J. He and W. C. Wimley, *Trends in Biochemical Sciences*, 2015, **40**, 749–764.

[19] A. R. Hilgers, R. A. Conradi and P. S. Burton, *Pharmaceutical Research: An Official Journal of the American Association of Pharmaceutical Scientists*, 1990, **7**, 902–910.

[20] T. D. Brown, K. A. Whitehead and S. Mitragotri, *Nature Reviews Materials*, 2020, **5**, 127–148.

[21] S. R. Hwang and Y. Byun, *Expert Opinion on Drug Delivery*, 2014, **11**, 1955–1967.

[22] S. N. Steinway, J. Saleh, B. K. Koo, D. Delacour and D. H. Kim, *Frontiers in Bioengineering and Biotechnology*, 2020, **8**, year.

[23] Q. Zhu, Z. Chen, P. K. Paul, Y. Lu, W. Wu and J. Qi, *Acta Pharmaceutica Sinica B*, 2021.

[24] Y. Han, Z. Gao, L. Chen, L. Kang, W. Huang, M. Jin, Q. Wang and Y. H. Bae, *Acta Pharmaceutica Sinica B*, 2019, **9**, 902–922.

[25] M. Liu, J. Zhang, W. Shan and Y. Huang, *Asian Journal of Pharmaceutical Sciences*, 2014, **10**, 275–282.

[26] Y. Yun, Y. W. Cho and K. Park, *Advanced Drug Delivery Reviews*, 2013, **65**, 822–832.

[27] A. MacAdam, *Advanced Drug Delivery Reviews*, 1993, **11**, year.

[28] Y. Xu, N. Shrestha, V. Préat and A. Beloqui, *Journal of Controlled Release*, 2020, **322**, 486–508.

[29] M. Kristensen and H. M. Nielsen, *Basic and Clinical Pharmacology and Toxicology*, 2016, **118**, 99–106.

[30] B. Albert, *Molecular Biology of the Cell*, WW Norton & Co, United States, 6th edn., 2015, pp. 200–400.

[31] M. A. Odenwald and J. R. Turner, *Nature Reviews Gastroenterology and Hepatology*, 2017, **14**, 9–21.

[32] A. Buckley and J. R. Turner, *Cold Spring Harbor Perspectives in Biology*, 2018, **10**, —.

[33] B. C. Doak, B. Over, F. Giordanetto and J. Kihlberg, in *Chemistry and Biology*, Elsevier Ltd, 2014, vol. 21, pp. 1115–1142.

[34] S. K. Dubey, S. Parab, N. Dabholkar, M. Agrawal, G. Singhvi, A. Alexander, R. A. Bapat and P. Kesharwani, *Drug Discovery Today*, 2021, **26**, —.

[35] C. A. Lipinski, F. Lombardo, B. W. Dominy and P. J. Feeney, *Advanced Drug Delivery Reviews*, 2001, **46**, 3–26.

[36] S. Verma, U. K. Goand, A. Husain, R. A. Katekar, R. Garg and J. R. Gayen, *Drug Development Research*, 2021.

[37] A. Ritzén and L. David, in *Successful Drug Discovery*, Wiley, 2019.

[38] K. Whitehead, N. Karr and S. Mitragotri, *Pharmaceutical Research*, 2008, **25**, —.

[39] S. Jafari, S. M. Dizaj and K. Adibkia, *BioImpacts*, 2015, **5**, 103–111.

[40] R. Ismail and I. Csóka, *Novel strategies in the oral delivery of antidiabetic peptide drugs – Insulin, GLP 1 and its analogs*, 2017.

[41] L. YH and S. PJ, *Advanced drug delivery reviews*, 2000, **42**, 225–238.

[42] M. A. Karsdal, K. Henriksen, A. C. Bay-Jensen, B. Molloy, M. Arnold, M. R. John, I. Byrjalsen, M. Azria, B. J. Riis, P. Qvist and C. Christiansen, *The Journal of Clinical Pharmacology*, 2011, **51**, 460–471.

[43] M. MJ, *Current osteoporosis reports*, 2012, **10**, 80–85.

[44] Y. Sambuy, I. De Angelis, G. Ranaldi, M. L. Scarino, A. Stammati and F. Zucco, *Cell Biology and Toxicology*, 2005, **21**, 1–26.

[45] I. Behrens and T. Kissel, *European Journal of Pharmaceutical Sciences*, 2003, **19**, 433–442.

[46] ATCC, *Caco-2*, 2021, https://www.atcc.org/products/htb-37.

[47] A. A. Akhtar, S. Sances, R. Barrett and J. J. Breunig, *Current Stem Cell Reports*, 2017, **3**, 98–111.

[48] C. Probst, S. Schneider and P. Loskill, *Current Opinion in Biomedical Engineering*, 2018, **6**, 33–41.

[49] J. Costa and A. Ahluwalia, *Frontiers in Bioengineering and Biotechnology*, 2019, **7**, year.

[50] C. Tian, Q. Tu, W. Liu and J. Wang, *TrAC - Trends in Analytical Chemistry*, 2019, **117**, 146–156.

[51] D. Huh, G. A. Hamilton and D. E. Ingber, *Trends in Cell Biology*, 2011, **21**, 745–754.

[52] V. van Duinen, S. J. Trietsch, J. Joore, P. Vulto and T. Hankemeier, *Current Opinion in Biotechnology*, 2015, **35**, 118–126.

[53] P. A. Billat, E. Roger, S. Faure and F. Lagarce, *Drug Discovery Today*, 2017, **22**, 761–775.

[54] N. S. Bhise, J. Ribas, V. Manoharan, Y. S. Zhang, A. Polini, S. Massa, M. R. Dokmeci and A. Khademhosseini, *Journal of Controlled Release*, 2014, **190**, 82–93.

[55] A. Bein, W. Shin, S. Jalili-Firoozinezhad, M. H. Park, A. Sontheimer-Phelps, A. Tovaglieri, A. Chalkiadaki, H. J. Kim and D. E. Ingber, *CMGH*, 2018, **5**, 659–668.

[56] B. Kramer, L. d. Haan, M. Vermeer, T. Olivier, T. Hankemeier, P. Vulto, J. Joore and H. L. Lanz, *International Journal of Molecular Sciences*, 2019, **20**, 4647.

[57] S. J. Trietsch, E. Naumovska, D. Kurek, M. C. Setyawati, M. K. Vormann, K. J. Wilschut, H. L. Lanz, A. Nicolas, C. P. Ng, J. Joore, S. Kustermann, A. Roth, T. Hankemeier, A. Moisan and P. Vulto, *Nature Communications*, 2017, **8**, 1–8.

[58] C. Beaurivage, A. Kanapeckaite, C. Loomans, K. S. Erdmann, J. Stallen and R. A. Janssen, *Scientific Reports*, 2020, **10**, 1–16.

[59] *Our Technology*, https://www.mimetas.com/en/our-technology/.

[60] M. K. Vormann, L. Gijzen, S. Hutter, L. Boot, A. Nicolas, A. van den Heuvel, J. Vriend, C. P. Ng, T. T. Nieskens, V. van Duinen, B. de Wagenaar, R. Masereeuw, L. Suter-Dick, S. J. Trietsch, M. Wilmer, J. Joore, P. Vulto and H. L. Lanz, *AAPS Journal*, 2018, **20**, 1–11.

[61] M. Wilson, *Introduction to Widefield Microscopy — Learn & Share — Leica Microsystems*, https://www.leica-microsystems.com/science-lab/introduction-to-widefield-microscopy/.

[62] D. B. Murphy and M. W. Davidson, *Fundamentals of Light Microscopy and Electronic Imaging*, John Wiley & Sons, Inc, 2nd edn., 2013.

[63] J. Oreopoulos, R. Berman and M. Browne, *Methods in Cell Biology*, 2014, **123**, 153–175.

[64] P. W. Hawkes and J. C. H. Spence, *Springer Handbook of Microscopy*, Springer International Publishing, Cham, 2019.

[65] S. Stehbens, H. Pemble, L. Murrow and T. Wittmann, 2012.

[66] L. Gijzen, D. Marescotti, E. Raineri, A. Nicolas, H. L. Lanz, D. Guerrera, R. van Vught, J. Joore, P. Vulto, M. C. Peitsch, J. Hoeng, G. Lo Sasso and D. Kurek, *SLAS Technology*, 2020, **25**, 585–597.